Modeling and simulation of neuronal morphology

Shin Ishii

Kyoto University

RIKEN Computational Research Program
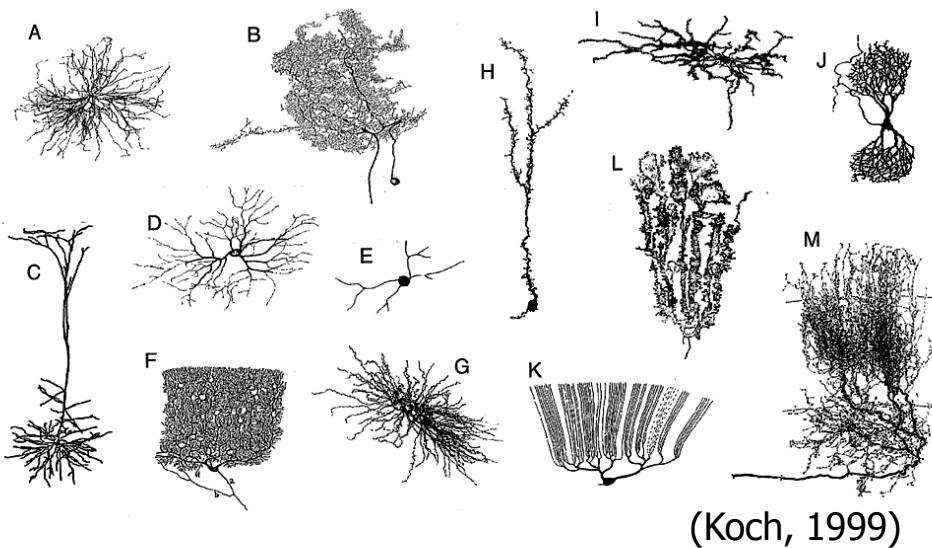
ATR Neural Information Analysis Laboratories
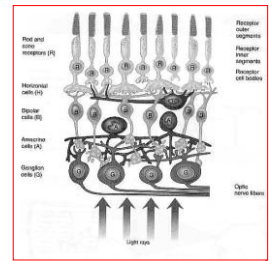
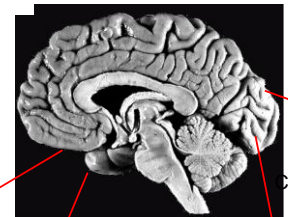# Morphological divergence of neurons

Basic hypothesis:

Morphology and structure are information representation in the brain.

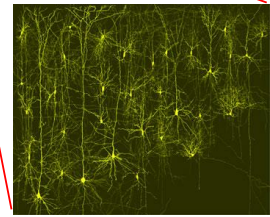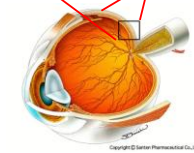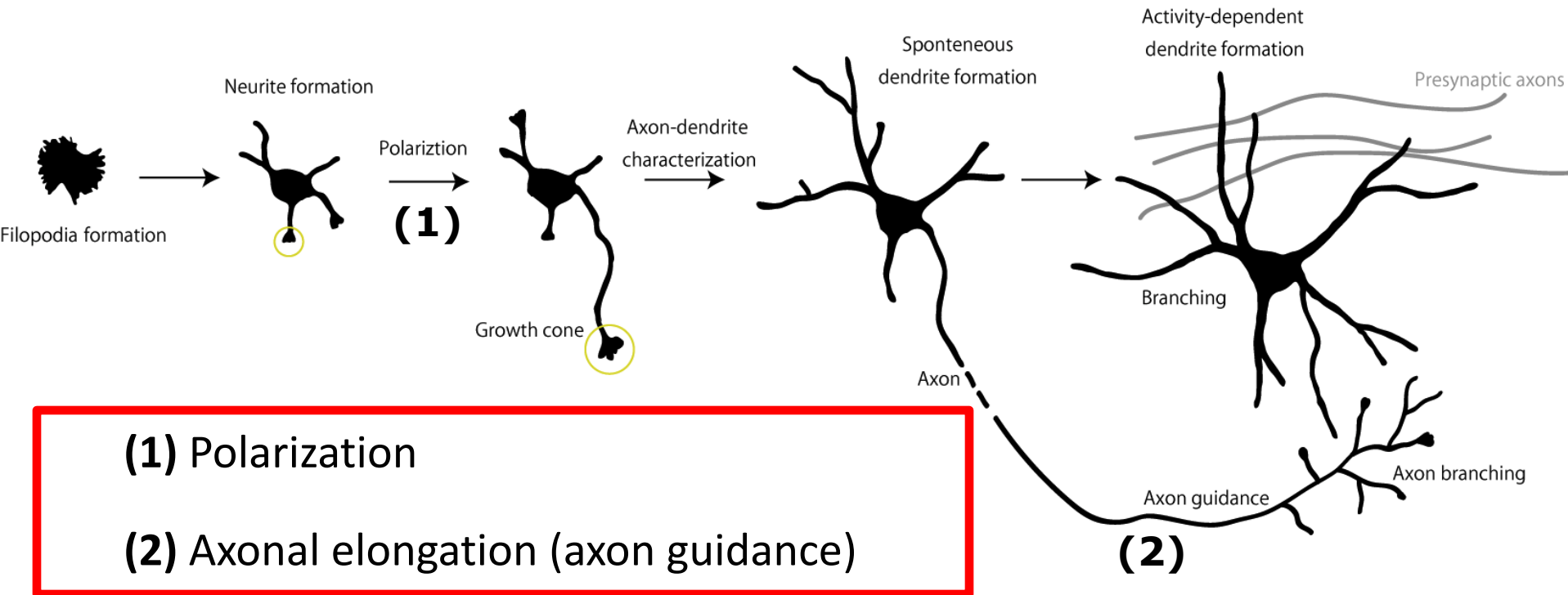

(Koch, 1999)

Ganglion, Bipolar, Rod,…

Cortical pyramidal neurons

Development process in the brain

How do neurons obtain their morphology?
How do neural circuits form their patterns?

Structural plasticity in neural development

Filopodia formation

Neurite formation

Polariztion

(1)

Growth cone

Axon-dendrite characterization

Sponteneous dendrite formation

Activity-dependent dendrite formation

Presynaptic axons

Branching

Axon

Axon guidance

Axon branching

(2)

> **(1)** Polarization
>
> **(2)** Axonal elongation (axon guidance)

- A decoding process from analog (and sometimes weak) molecular signals to digital morphology
- Can be symmetry breaking phenomena

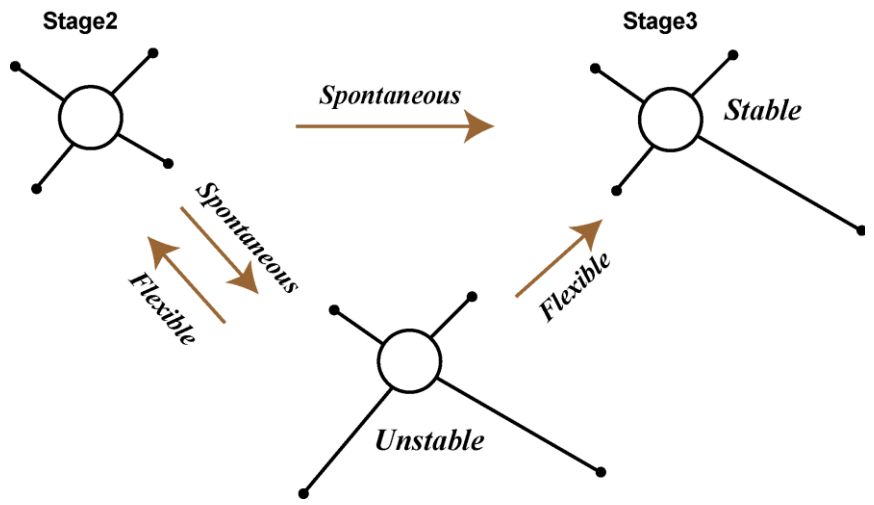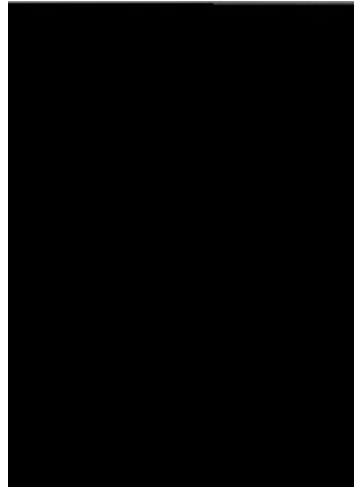# Spontaneous neuronal polarization: model, mathematics and biology

Naoki, H., Nakamuta, S., Kaibuchi, K., Ishii, S. PLoS ONE, 6, 2011.
Toriyama, M., Sakumura, Y., Shimada, T., Ishii, S., Inagaki, N.
Molecular Systems Biology, 6, 2010.

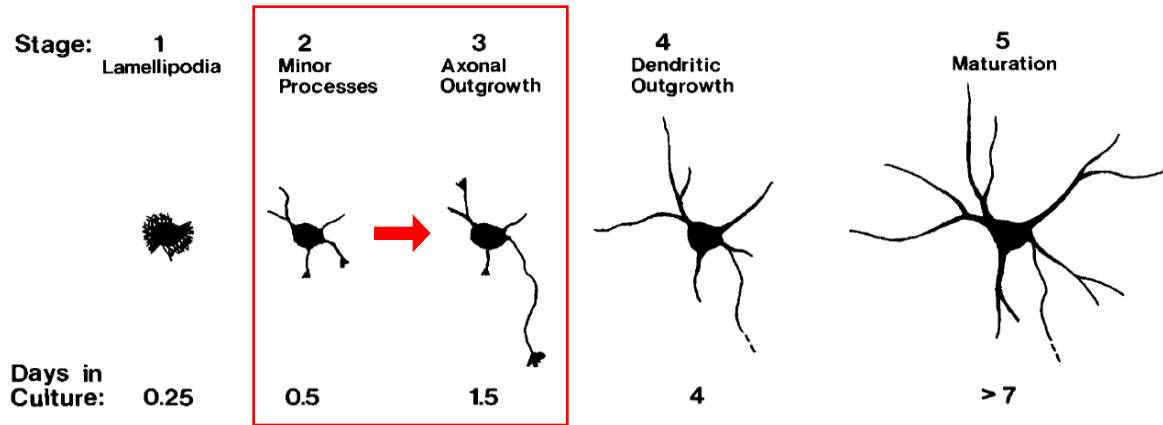# Axon determination of differentiated neurons
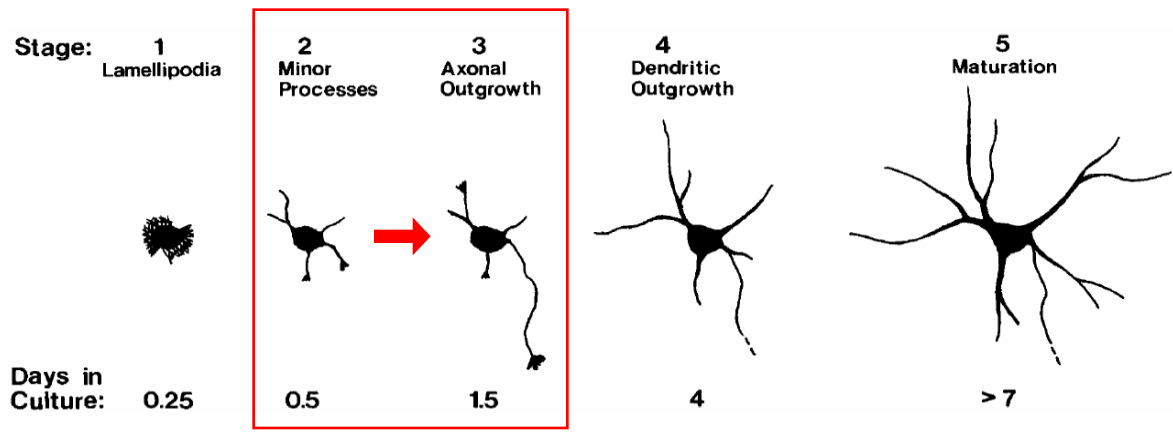
Dotti et. al, J Neurosci, 1988

from website of Banker Lab

- **Spontaneity**
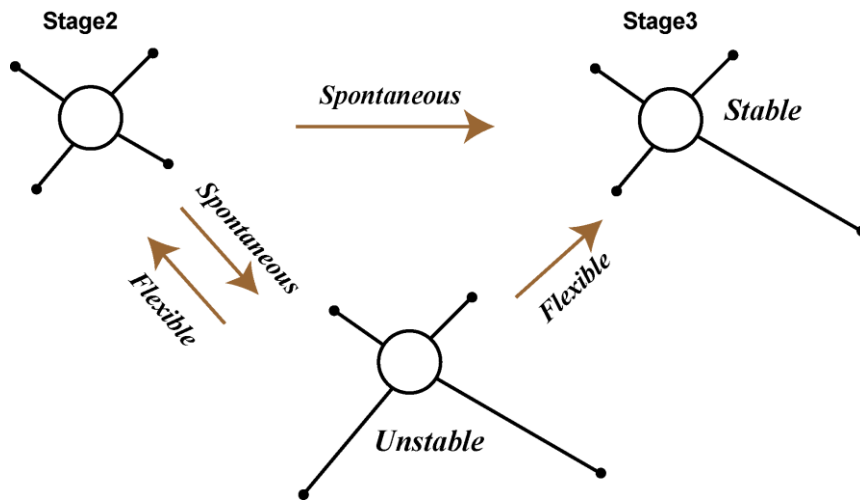 A neuron is *spontaneously* polarized, even in a uniform extracellular condition.

Axon determination of differentiated neurons

Dotti et. al, J Neurosci, 1988

from website of Banker Lab

- **Spontaneity**
  A neuron is *spontaneously* polarized, even in an uniform extracellular condition.

- **Stabilization**
  Once a single axon is selected, remaining neurites cannot be elongated.

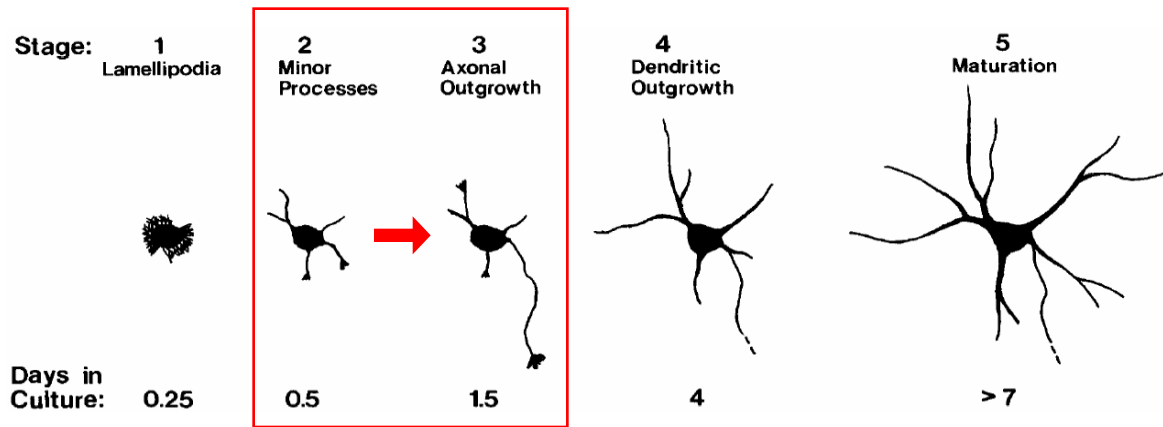# Axon determination of differentiated neurons

Dotti et. al, J Neurosci, 1988
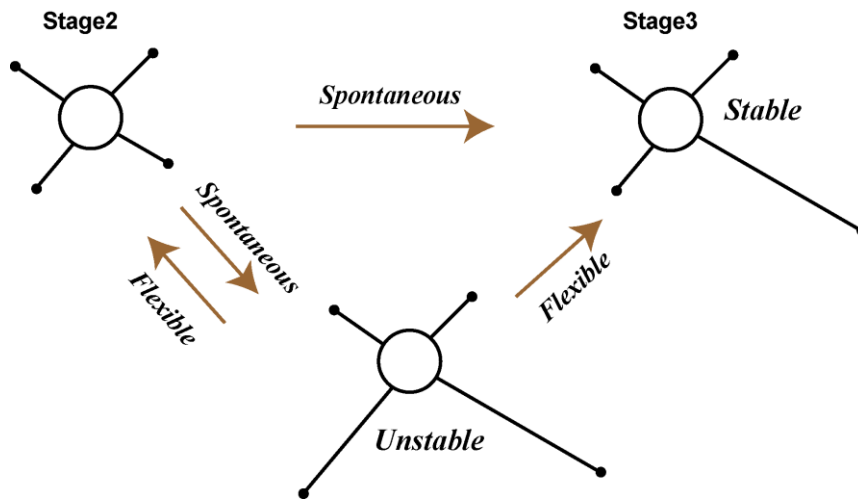

from website of Banker Lab

- **Spontaneity**
  A neuron is *spontaneously* polarized, even in an uniform extracellular condition.

- **Stabilization**
  Once a single axon is selected, remaining neurites cannot be elongated.

- **Correction**
  Sometime, multiple neurites mistakenly happen to be selected, but this failed pattern is *flexibly* cancelled out to yield a single axon.

What is the mechanism of such a flexible morphogenesis?

Model: axon determination molecule

- ## Compartment model
  - ### Soma, several neurites
- Axon determination molecule: factor X
  - Gene expression in the soma
  - Degradation or inactivation
  - Diffusion
  - Active transport from the soma to each neurite tip

ODE (Concentration of factor X **in the soma**)

$$\frac{dC_s}{dt} = G - kC_s + \frac{1}{V}\sum_i^N \left[DA\frac{\partial C_i(0,t)}{\partial x} - \alpha C_s \right]$$

PDE (Concentration of factor X **along each neurite**)

$$\frac{\partial C_i}{\partial t} = D\frac{\partial^2 C_i}{\partial x^2} - kC_i - D\frac{\partial C_i(0,t)}{\partial x}\delta(0) + \frac{\alpha C_s}{A}\delta(L_i)$$

Growth cone

$L_i(\mu m)$

$C_i(x,t)$

$C_s(t)$

Active Transport

Passive Diffusion

Model: axon determination molecule

- Compartment model
  - Soma, several neurites
- Axon determination molecule: factor X
  - Gene expression in the soma
  - Degradation of inactivation
  - Diffusion
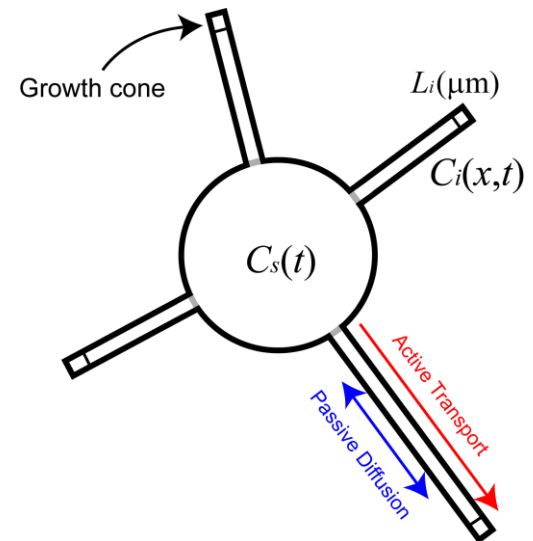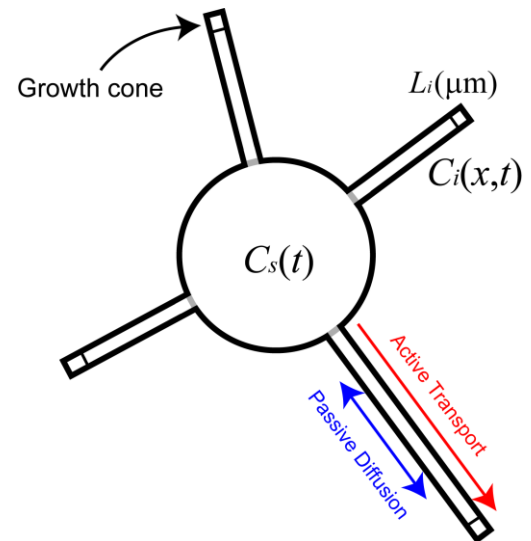 - Active transport from the soma to each neurite tip

ODE (Concentration of factor X **in the soma**)

$$\frac{dC_s}{dt} = \boxed{G} - \boxed{kC_s} + \frac{1}{V}\sum_i^N \left[DA \frac{\partial C_i(0,t)}{\partial x} - \alpha C_s \right]$$

PDE (Concentration of factor X **along each neurite**)

$$\frac{\partial C_i}{\partial t} = D \frac{\partial^2 C_i}{\partial x^2} \boxed{- kC_i} - D \frac{\partial C_i(0,t)}{\partial x}\delta(0) + \frac{\alpha C_s}{A}\delta(L_i)$$

Growth cone

$L_i(\mu m)$

$C_i(x,t)$

$C_s(t)$

Active Transport

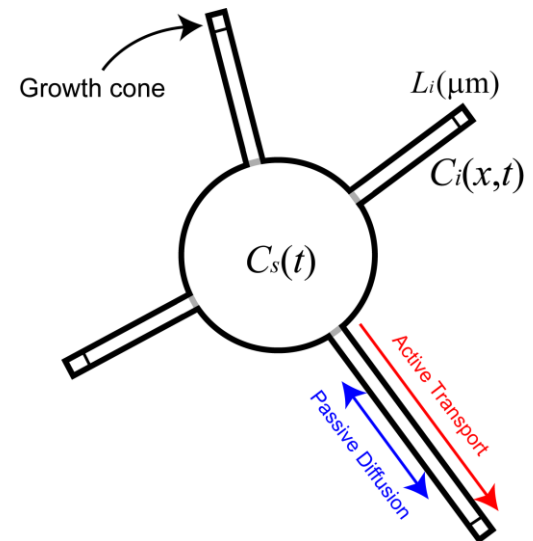Passive Diffusion

Model: axon determination molecule

- Compartment model
  - Soma, several neurites
- Axon determination molecule: factor X
  - Gene expression in the soma
  - Degradation or inactivation
  - Diffusion
  - Active transport from the soma to each neurite tip

ODE (Concentration of factor X **in the soma**)

$$\frac{dC_s}{dt} = G - kC_s + \frac{1}{V}\sum_i^N \left[\boxed{DA\frac{\partial C_i(0,t)}{\partial x}} - \alpha C_s \right]$$

PDE (Concentration of factor X **along each neurite**)

$$\frac{\partial C_i}{\partial t} = \boxed{D\frac{\partial^2 C_i}{\partial x^2}} - kC_i \boxed{- D\frac{\partial C_i(0,t)}{\partial x}\delta(0)} + \frac{\alpha C_s}{A}\delta(L_i)$$

Growth cone

$L_i(\mu m)$

$C_i(x,t)$

$C_s(t)$

Active Transport

Passive Diffusion

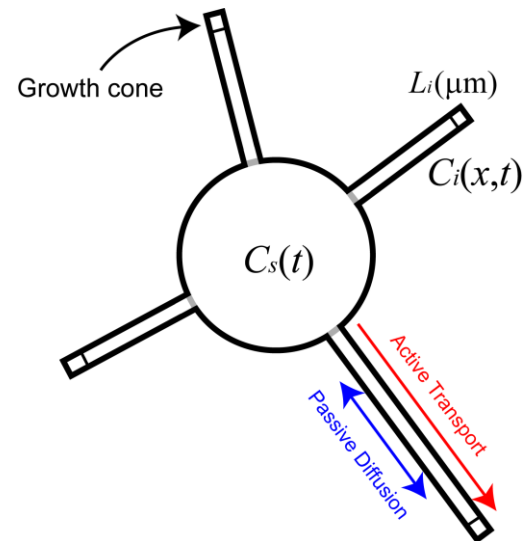# Model: axon determination molecule

- Compartment model
  - Soma, several neurites
- Axon determination molecule: factor X
  - Gene expression in the soma
  - Degradation or inactivation
  - Diffusion
  - Active transport from the soma to each neurite tip
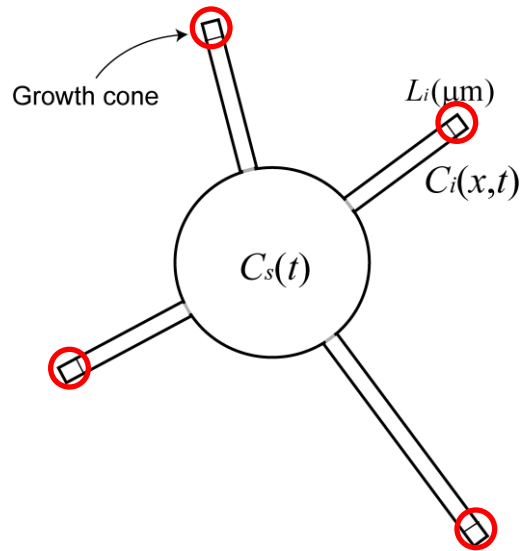
ODE (Concentration of factor X **in the soma**)

$$\frac{dC_s}{dt} = G - kC_s + \frac{1}{V} \sum_i^N \left[DA \frac{\partial C_i(0,t)}{\partial x} \boxed{-\alpha C_s} \right]$$

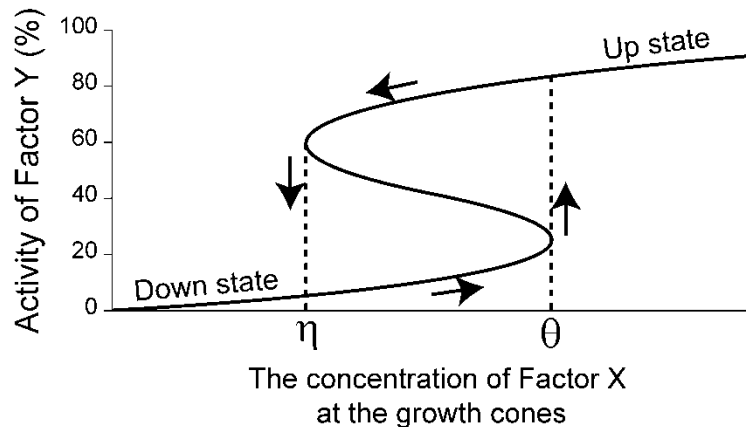PDE (Concentration of factor X **along each neurite**)

$$\frac{\partial C_i}{\partial t} = D \frac{\partial^2 C_i}{\partial x^2} - kC_i - D \frac{\partial C_i(0,t)}{\partial x} \delta(0) \boxed{+ \frac{\alpha C_s}{A} \delta(L_i)}$$
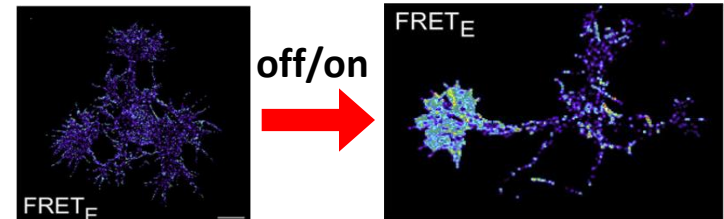
Growth cone

$L_i(\mu m)$

$C_i(x,t)$

$C_s(t)$

Active Transport

Passive Diffusion

Model: cytoskeleton regulating molecule

Growth cone

$L_i (\mu m)$

$C_i(x,t)$

$C_s(t)$

- Cytoskeleton regulating molecule: factor Y
  - Work at each neurite tip
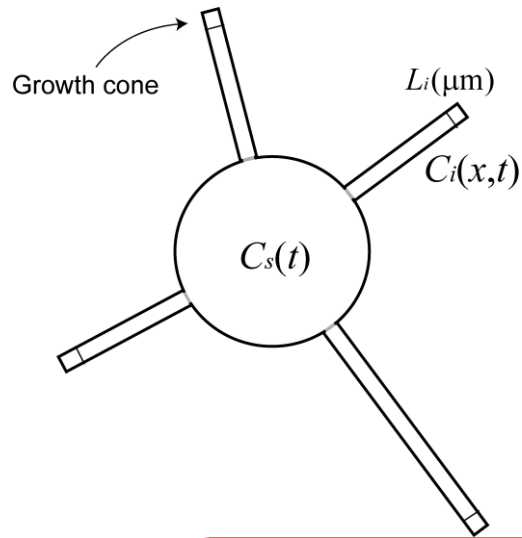 - Activated by the axon determination factor (X)
  - Bistable switch (hysteresis)

Activity of Factor Y (%)

Up state

Down state

η θ

The concentration of Factor X
at the growth cones

FRET$_E$ off/on   FRET$_E$

Fivaz et. al, Curr Biol, 2008

- When factor Y is "up state", neurite elongates.
- When factor Y is "down state", neurite shrinks.
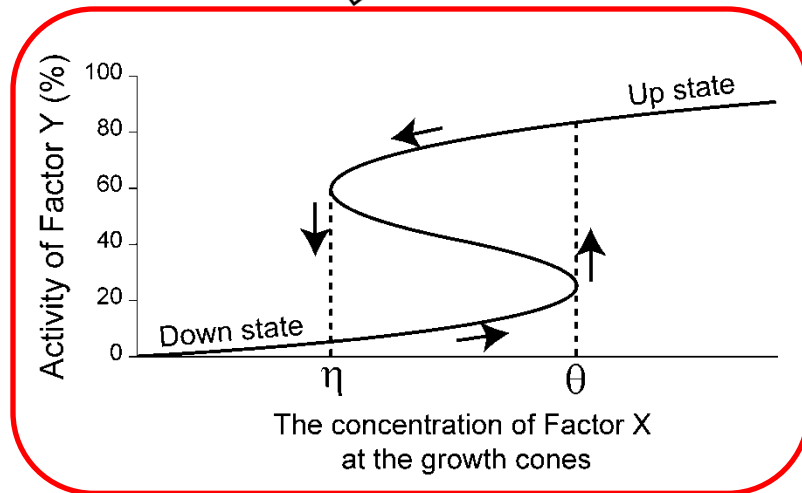
HRas behaves like a molecular switch, being highly activated in the selected neurite.

Model: cytoskeleton regulating molecule
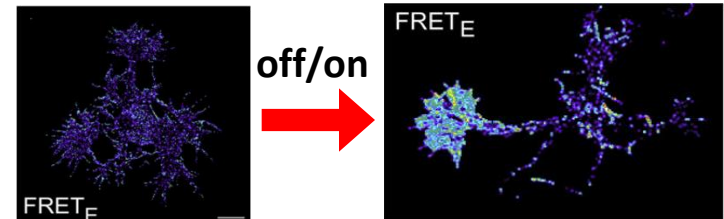
Growth cone

$L_i(\mu m)$

$C_i(x,t)$

$C_s(t)$

- Cytoskeleton regulating molecule: factor Y
  - Work at each neurite tip
  - Activated by the axon determination factor (X)
  - Bistable switch (hysteresis)

Activity of Factor Y (%)

Up state

Down state

η θ

The concentration of Factor X
at the growth cones

off/on

FRET$_E$

FRET$_E$

FRET$_E$

Fivaz et. al, Curr Biol, 2008

- When factor Y is "up state", neurite elongates.
- When factor Y is "down state", neurite shrinks.
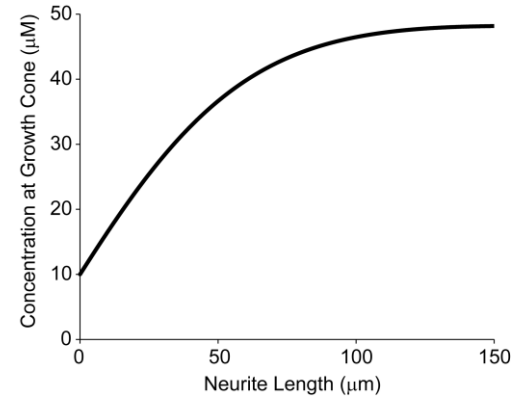
 HRas behaves like a molecular switch, being highly activated in the selected neurite.

Mathematics: Winner-take-all mechanism

- Local activation in the growth cone
  - Factor X is accumulated in the growth cone due to the increasing active transportation

- Global inhibition in the somatic pool
  - As the neurite becomes long, it is difficult for factor X to diffuse back to the soma.
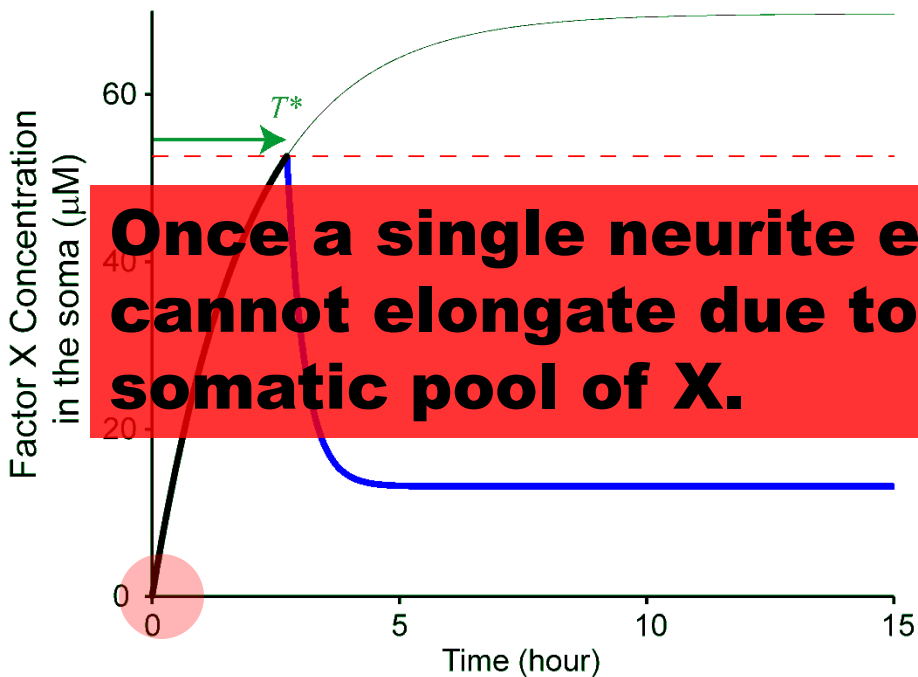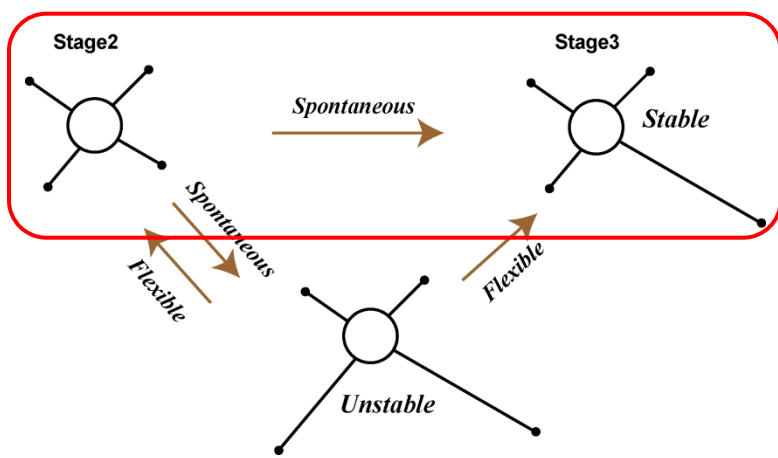 - If there are long neurites, the somatic pool of factor X is dried up.

$$C_i(L_i)=C_s\left[\frac{\alpha}{A\sqrt{kD}}\tanh\left(\sqrt{k/D}L_i\right)+\cosh\left(\sqrt{k/D}L_i\right)^{-1}\right]$$

$$\frac{dC_s}{dt}=-\frac{C_s-GQ^{-1}}{Q^{-1}}$$

$$Q(\{L_i\})=k+V^{-1}\sum_i^N\left[A\sqrt{kD}\tanh\left(\sqrt{k/D}L_i\right)+\alpha\lambda\{1-RB(L_i)\}\right]$$
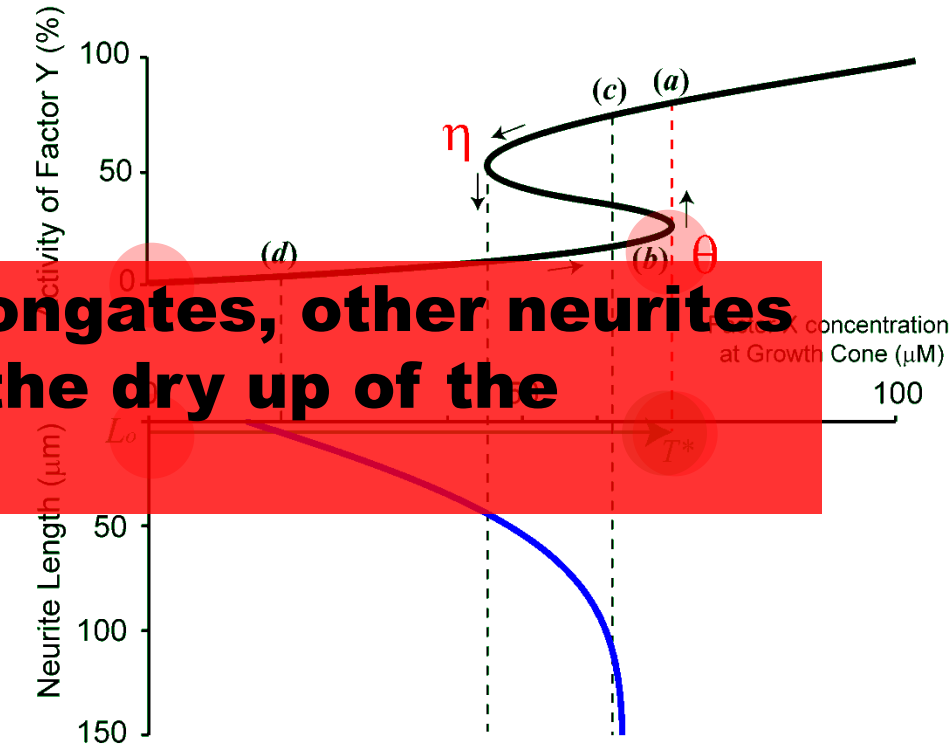
No long neurite
Single long neurite
Two long neurites
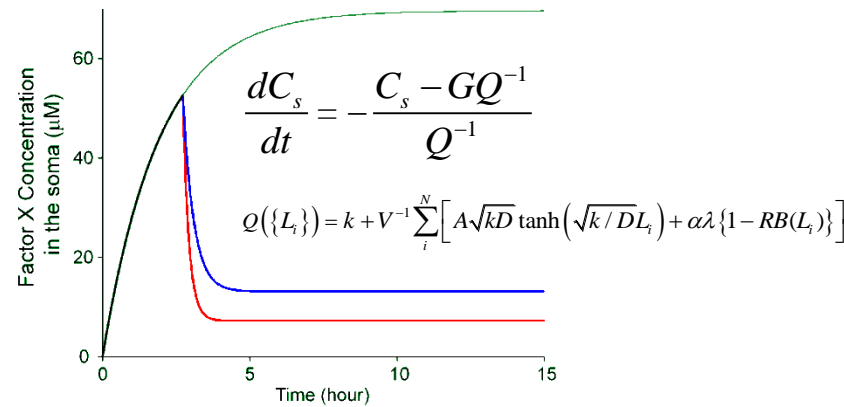
Mathematics:
Spontaneity and stability

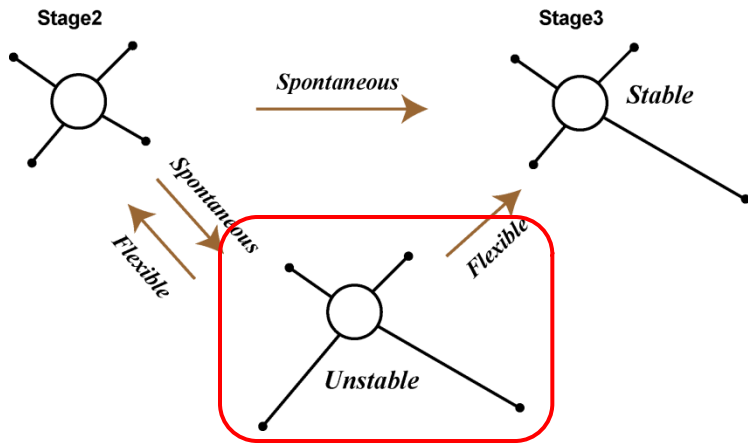**Activity of factor Y (depending on factor X)**

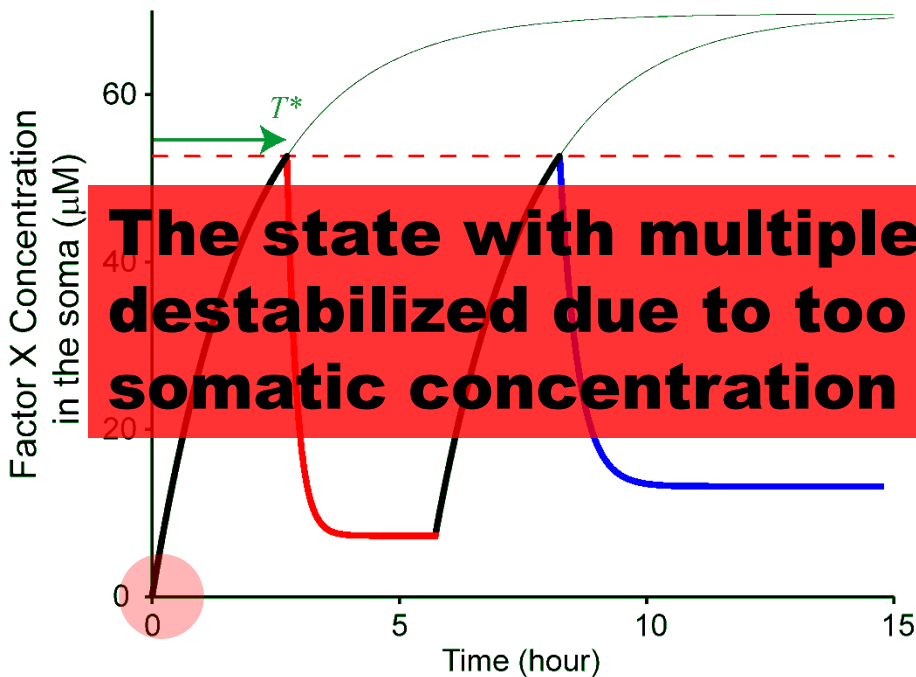Once a single neurite elongates, other neurites cannot elongate due to the dry up of the somatic pool of X.

Dynamics of factor X in the soma

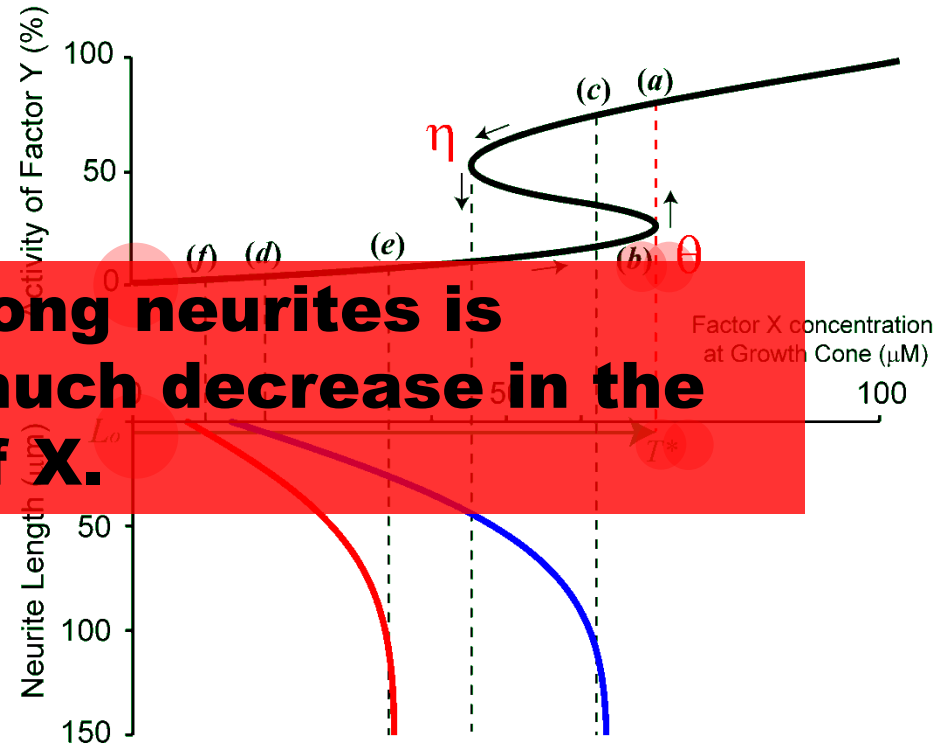**Concentration of factor X in the neurite tip vs Neurite length**

Mathematics: Correction

Stage2 → (Spontaneous) → Stage3 Stable

Spontaneous / Flexible — Unstable — Flexible

Activity of factor Y (depending on factor X)

Activity of Factor Y (%)

η

(c) (a)

(f) (d) (e) (b) θ

Factor X concentration at Growth Cone (μM)

100

Factor X Concentration in the soma (μM)

T^*

60

40

20

0

0   5   10   15

Time (hour)

Neurite Length (μm)

L_0 T^*

50

100

150

The state with multiple long neurites is destabilized due to too much decrease in the somatic concentration of X.
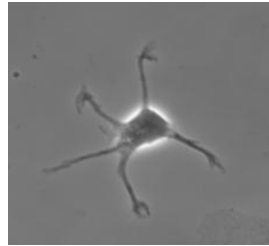
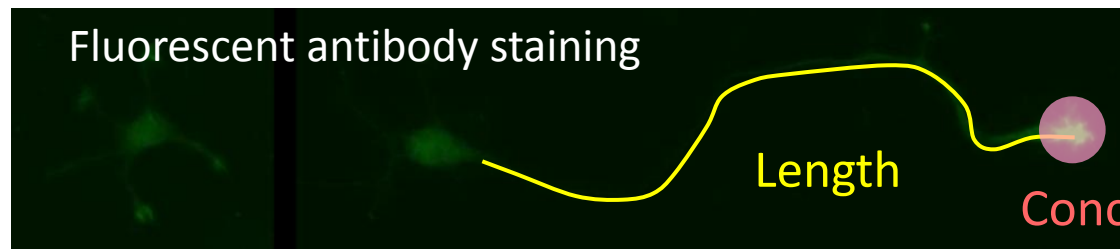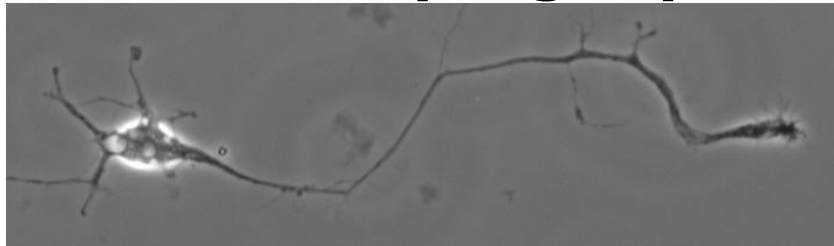**Dynamics of factor X in the soma**

Concentration of factor X in the neurite tip vs Neurite length

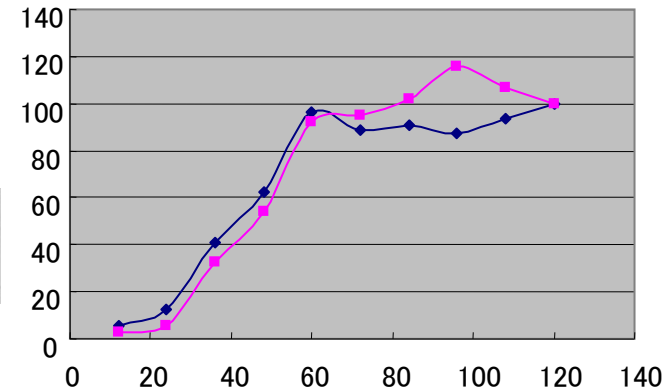# Biology: Neuronal polarization correlates with expression of Shootin1

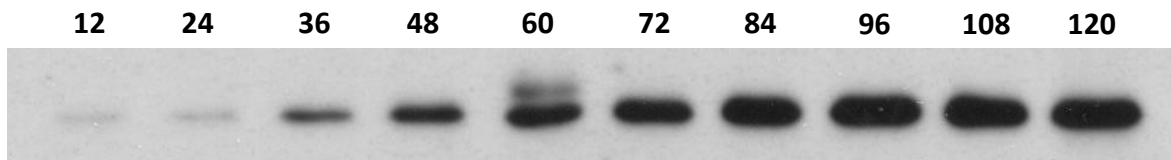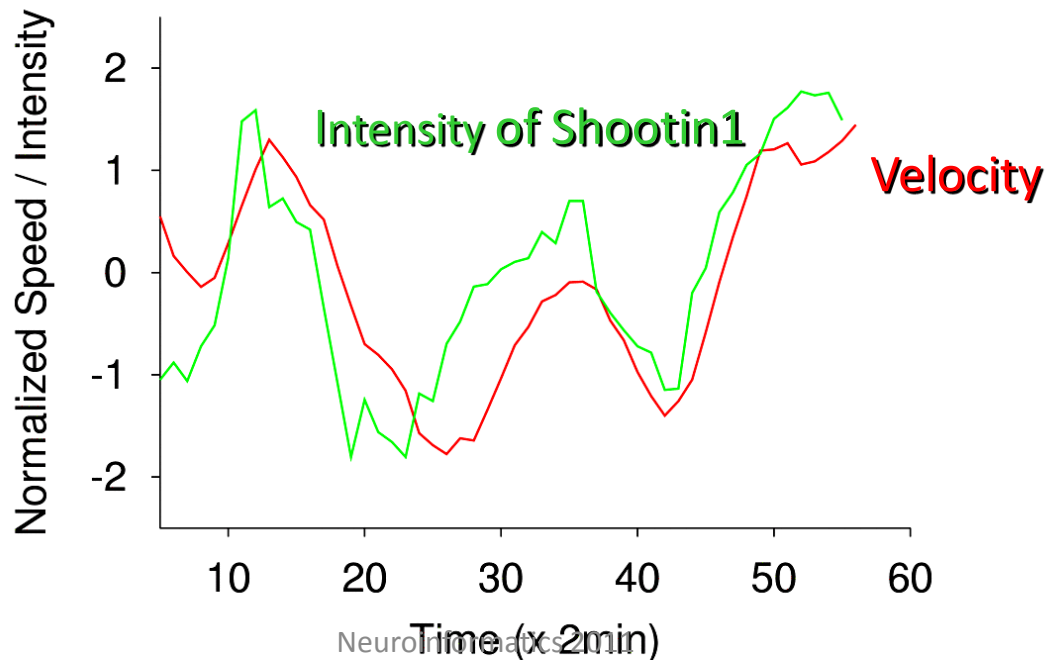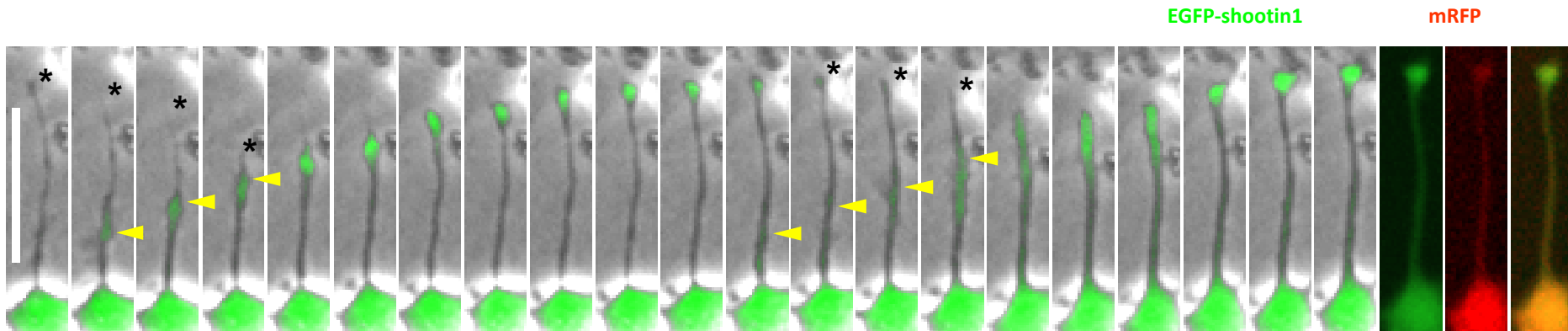**Before polarization (Stage 2)**

After polarization (Stage 3)

Fluorescent antibody staining

Length

Concentration

Expression rate of Shootin1

| 12 | 24 | 36 | 48 | 60 | 72 | 84 | 96 | 108 | 120 |

Biology: Active transportation of Shootin1

EGFP-shootin1   mRFP

Intensity of Shootin1

Velocity

Normalized Speed / Intensity

Time (x 2min)

NeuroInformatics 2011

Biology: Estimation of the diffusion constant of Shootin1

Kaede experiment

Before UV irradiation

Green Kaede-shootin1

Red Kaede-shootin1

After UV irradiation

55 min after UV irradiation
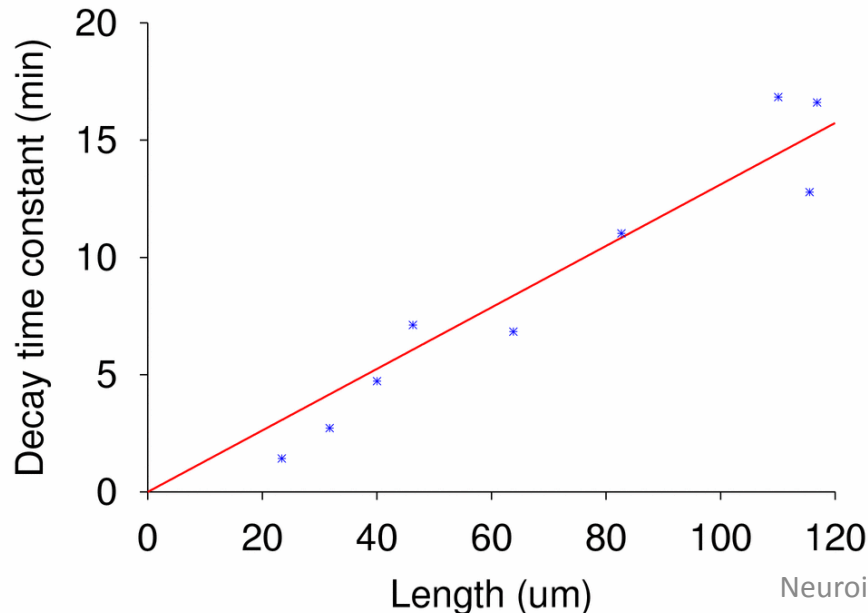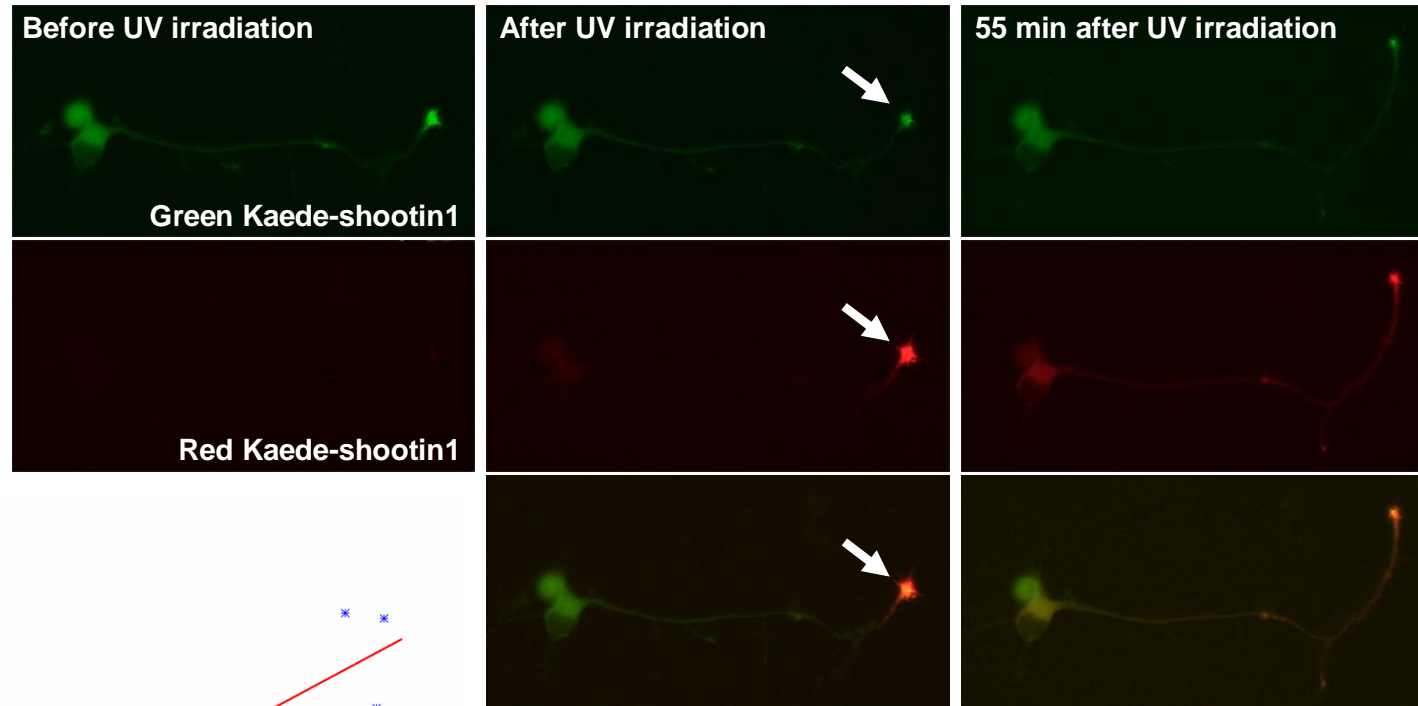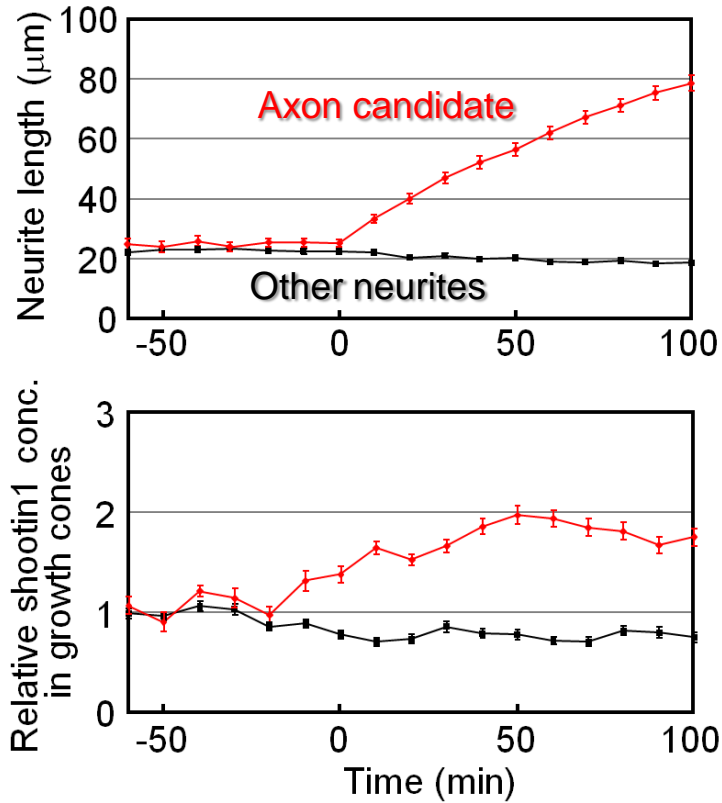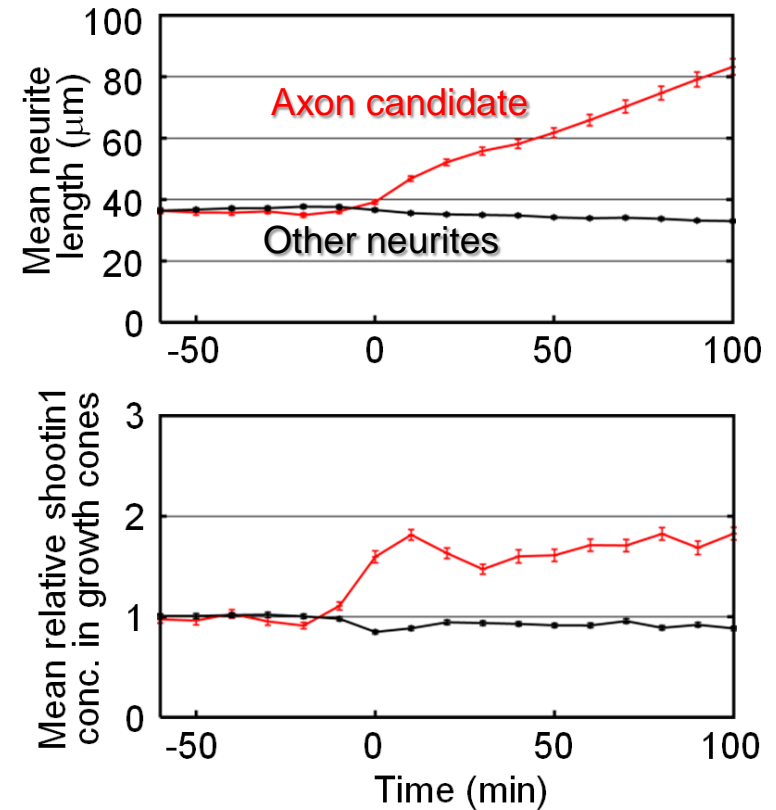
Based on the linear relationship between the neurite length and the decay time constant, we can estimate the diffusion constant.

Neuroinformatics 2011

Simulation: Outgrowth velocity dependent on Shootin1

Experiment vs. simulation

Average time-series(n=9)

Average time-series(n=50)
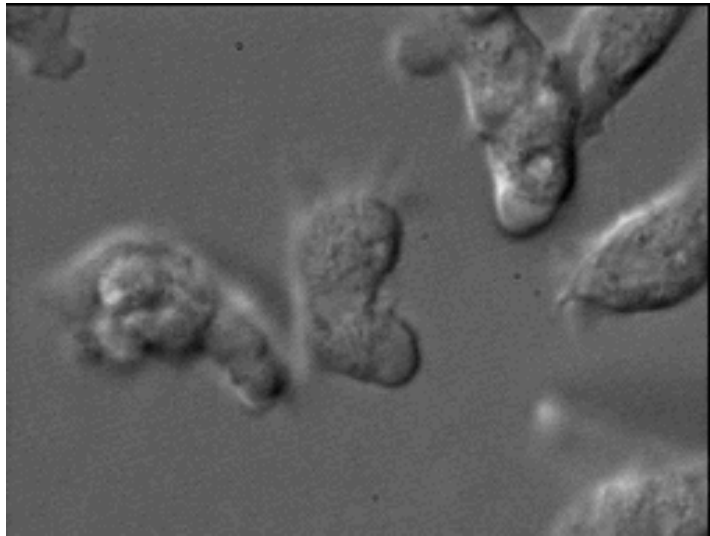
Experiment: primary cultured neurons

Computer simulation

High SNR in chemotaxis: model and mathematics

Naoki, H., Sakumura, Y., Ishii, S. Journal of Theoretical Biology, 2008.
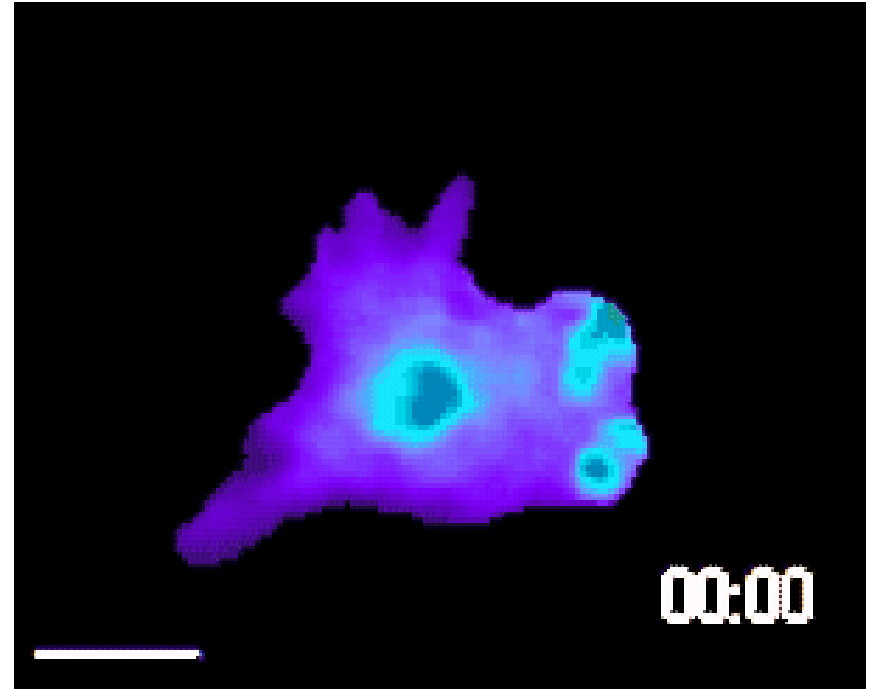
Spontaneous pulses in chemotactic cells

Chemotaxis is a property that a cell detects the gradient of chemical substance and moves up toward its direction.

A chemotactic cell of immune system

(Arrieumerlou et al, Dev Cell, 2005)

Cellular slime molds
(from Website of Yanagida Lab in Osaka Univ.)
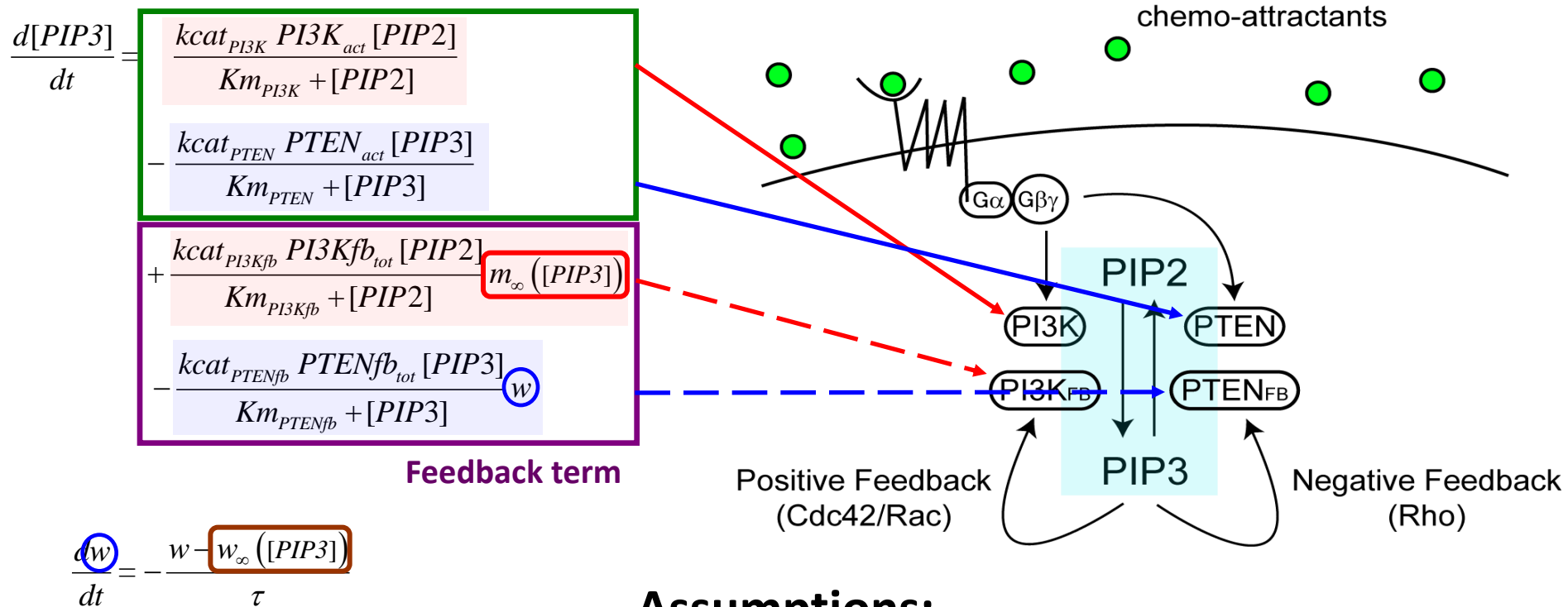
PIP3 pulse

Spontaneous and transient Increase in *PIP3* concentration leads to cellular elongation and determines moving direction.
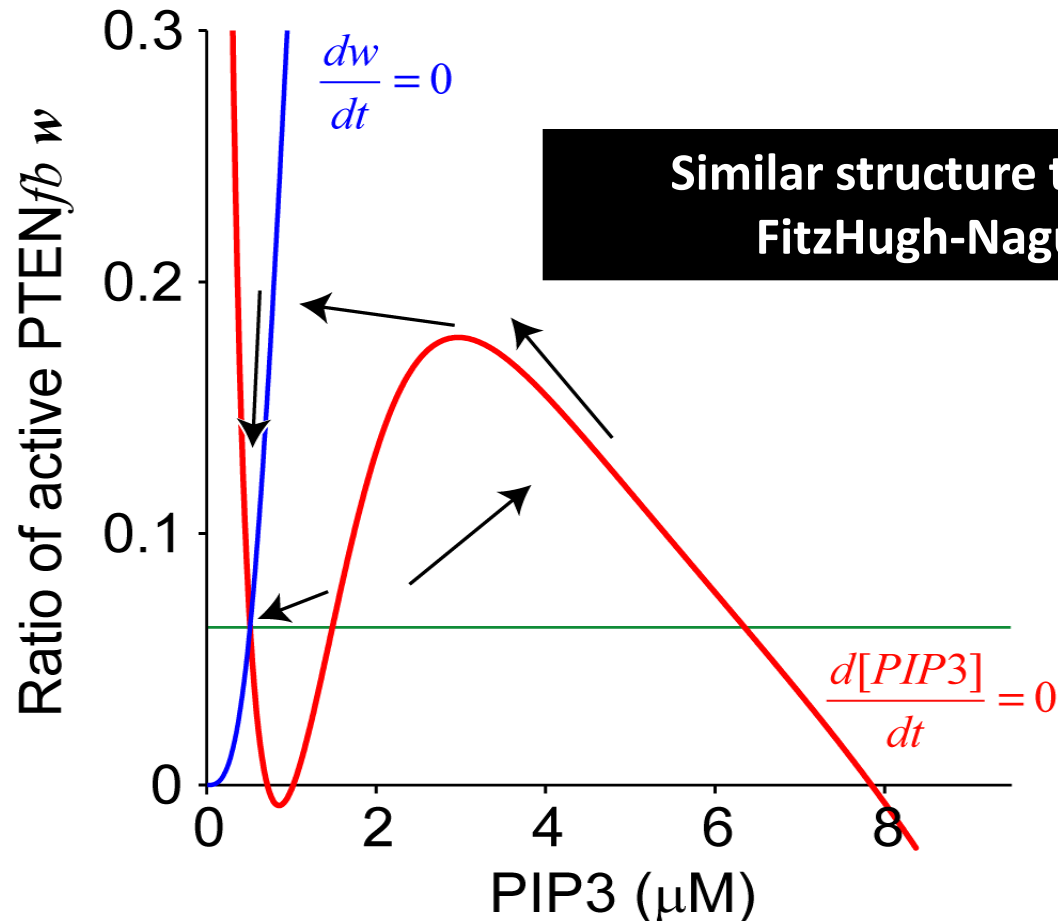
A biochemical model of PIP3 pulse generation

$$\frac{d[PIP3]}{dt} = \boxed{\begin{array}{c} \dfrac{kcat_{PI3K}\, PI3K_{act}\, [PIP2]}{Km_{PI3K} + [PIP2]} \\[2ex] -\dfrac{kcat_{PTEN}\, PTEN_{act}\, [PIP3]}{Km_{PTEN} + [PIP3]} \end{array}}$$

$$\boxed{\begin{array}{c} +\dfrac{kcat_{PI3Kfb}\, PI3Kfb_{tot}\, [PIP2]}{Km_{PI3Kfb} + [PIP2]}\, \boxed{m_\infty\big([PIP3]\big)} \\[2ex] -\dfrac{kcat_{PTENfb}\, PTENfb_{tot}\, [PIP3]}{Km_{PTENfb} + [PIP3]}\, \widehat{w} \end{array}}$$

Feedback term

$$\frac{dw}{dt} = -\frac{w - \boxed{w_\infty\big([PIP3]\big)}}{\tau}$$

$$where \quad PIP_{tot} = [PIP2] + [PIP3]$$

$$\boxed{m_\infty\big([PIP3]\big)} = \frac{[PIP3]^{h^{PI3K}}}{K_{PI3Kfb}{}^{h^{PI3K}} + [PIP3]^{h^{PI3K}}}$$

$$\boxed{w_\infty\big([PIP3]\big)} = \frac{[PIP3]^{h^{PTEN}}}{K_{PTENfb}{}^{h^{PTEN}} + [PIP3]^{h^{PTEN}}}$$

chemo-attractants

Gα Gβγ

PIP2

PI3K   PTEN

PI3K_FB   PTEN_FB

PIP3

Positive Feedback (Cdc42/Rac)

Negative Feedback (Rho)

Assumptions:

- **Positive feedback** is **fast** and then **chemically equilibrated**.

- **Negative feedback** is **slow**.

- Activities of *PI3Kfb* and *PTENfb* are provided by **Hill equations** of [*PIP3*].

- Total mass of PIP2 and PIP3 are constant.

PIP3 pathway constitutes an excitable system

Similar structure to the excitable FitzHugh-Nagumo model

$$\frac{dw}{dt} = 0$$

$$\frac{d[PIP3]}{dt} = 0$$

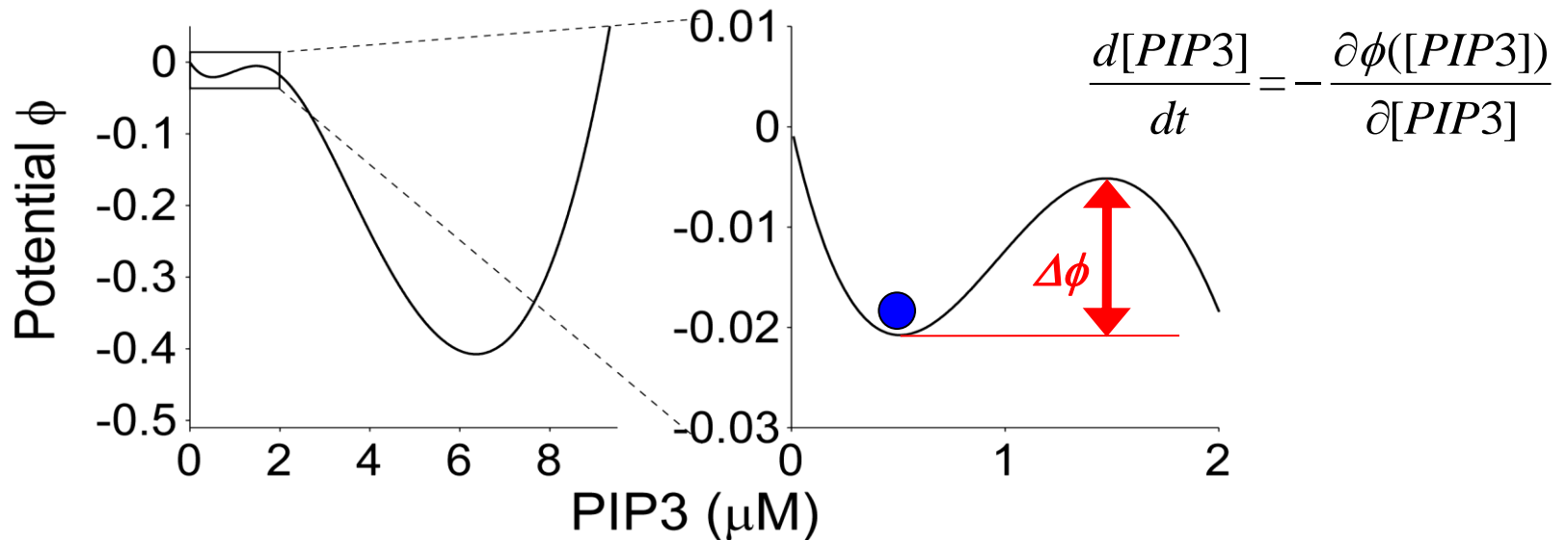Ratio of active PTENfb w

PIP3 (μM)

PIP3-related signal transduction consisting of positive and negative feedback loops can be an **excitable system**.

Mechanism of spontaneous signal generation

Brownian motion under potential field
(comprised by stochastic nature of chemical reactions)

Potential:

$$\frac{d[PIP3]}{dt} = -\frac{\partial \phi([PIP3])}{\partial [PIP3]}$$

Langevin equation

$$\frac{d[PIP3]}{dt} = -\frac{d\phi([PIP3])}{d[PIP3]} + \sqrt{2D}\xi$$

$$\langle \xi(t)\xi(t') \rangle = \delta(t - t')$$

Kramers transition rate   HA Kramers, Physica, 1940

$$k = \frac{\sqrt{\phi_s'' \cdot |\phi_{us}''|}}{2\pi} exp\left(-\frac{\Delta\phi}{D}\right)$$

_D_ : Diffusion constant in potential field
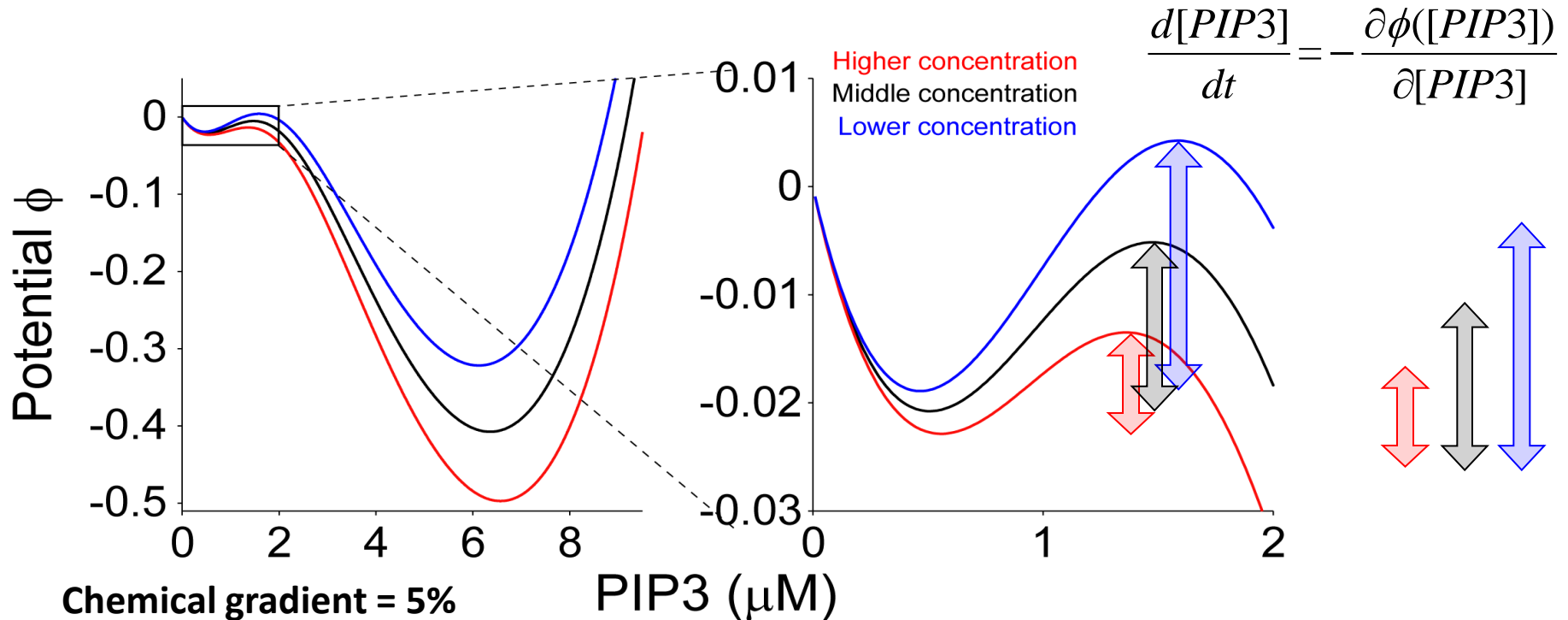
Nonlinear amplification of the linear gradient
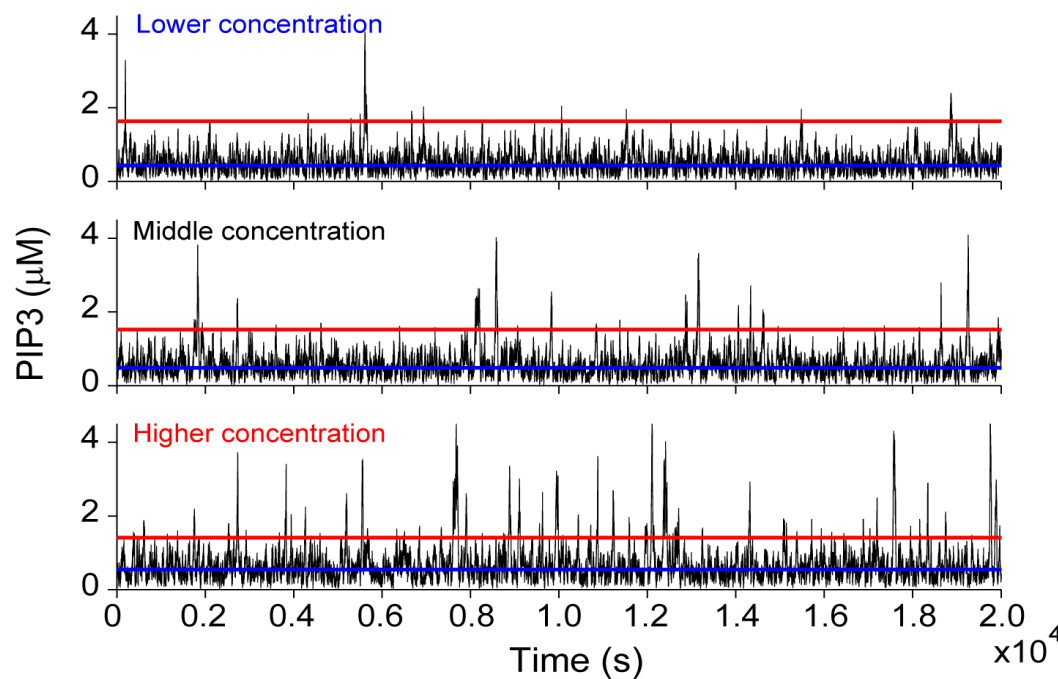
Chemical Gradient

cell

PI3K ↓
PTEN ↑

PI3K ↑
PTEN ↓

Lower
Concentration

Middle
Concentration

Higher
Concentration
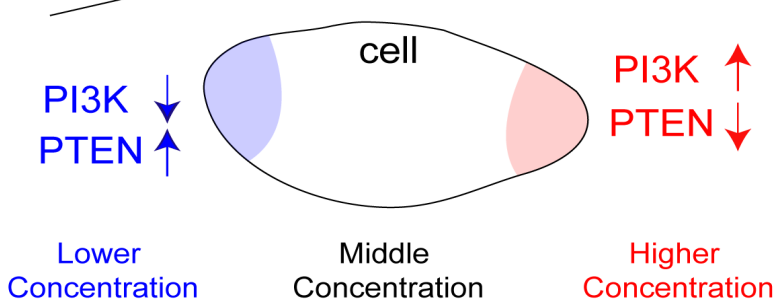
Chemical gradient are give as
localized accumulation of PI3K/PTEN
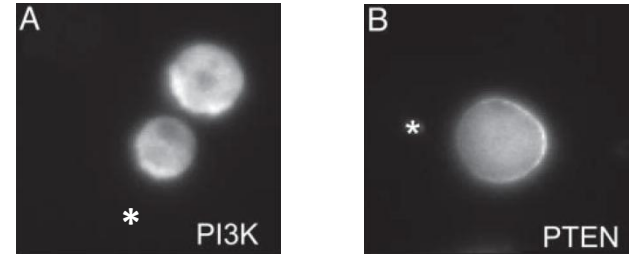
Janetopoulos et al, PNAS, 2004

$$\frac{d[PIP3]}{dt} = -\frac{\partial \phi([PIP3])}{\partial [PIP3]}$$

Higher concentration
Middle concentration
Lower concentration

Potential ϕ

PIP3 (μM)

Chemical gradient = 5%

Monte-Carlo simulation of the signal pathway reproduces the theoretical results
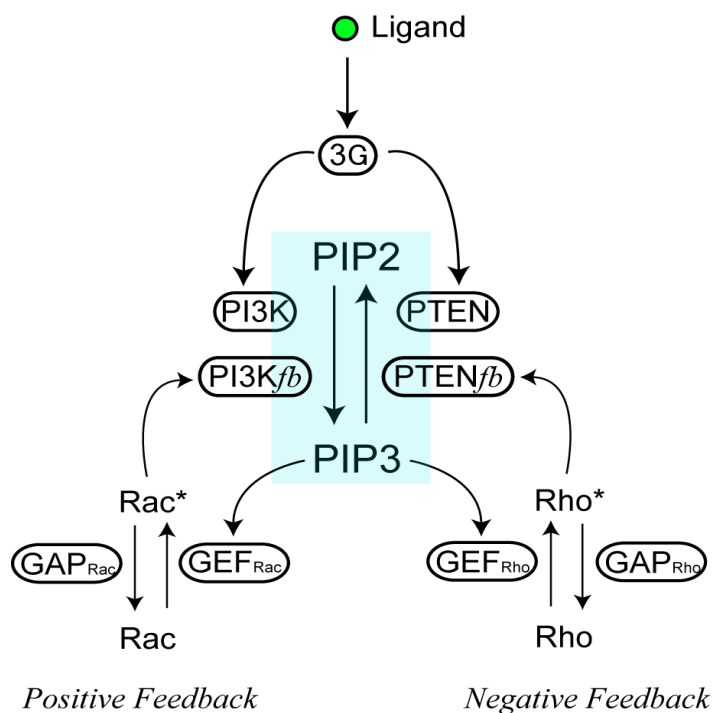
31 molecule kinds / 38 reactions

Monte-Carlo simulation

Bidirectional response by growth cones: biology and model

Nishiyama, M., Naoki, H., Ishii, S., Hong, K.
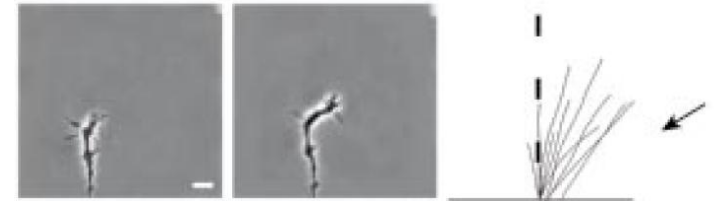
Bidirectional responses of growth cones
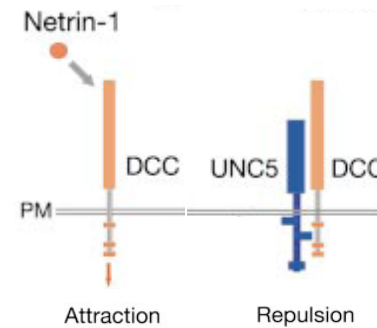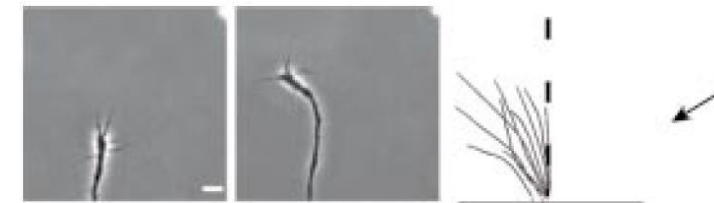

Filopodia

Lamellipodia
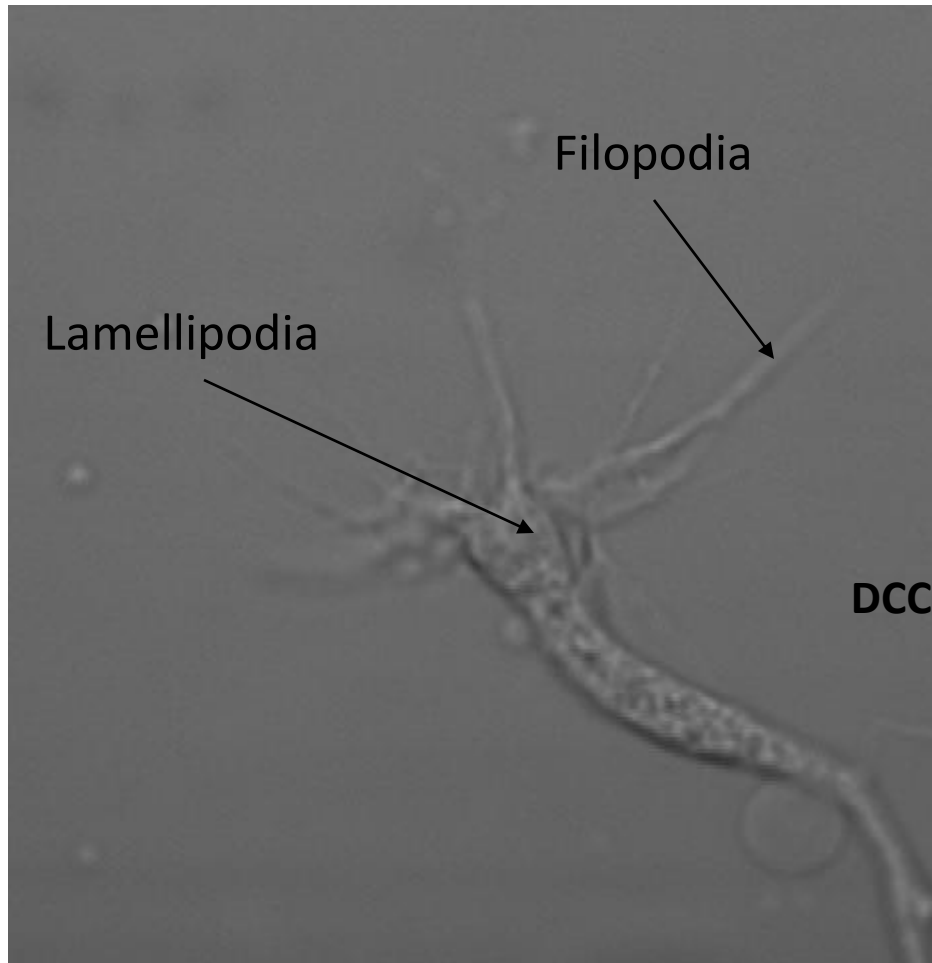
(*Xenopus* spinal neuron)

Receptor for cue molecule
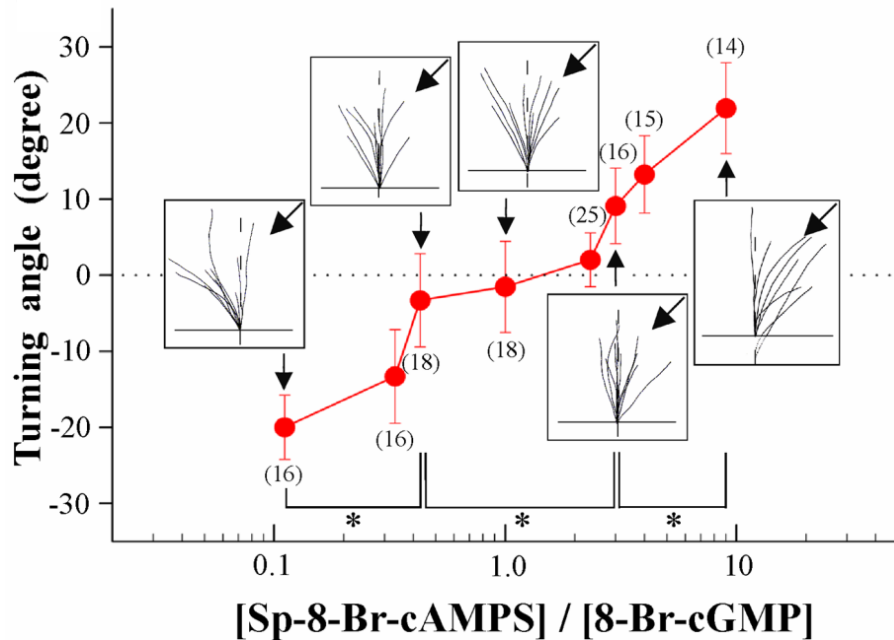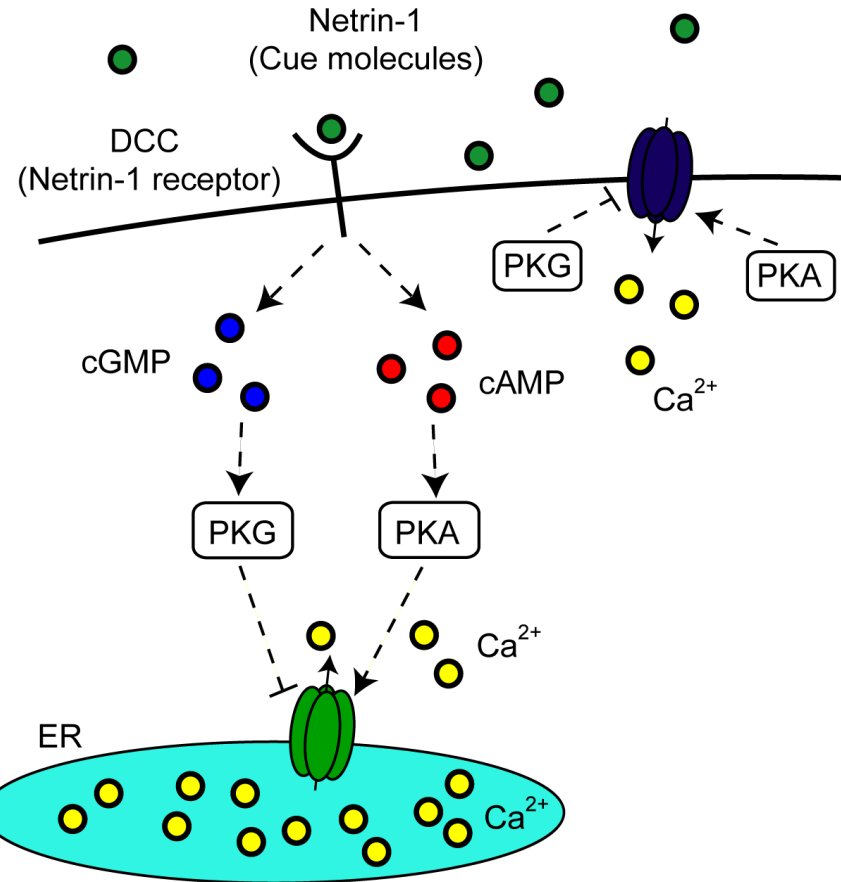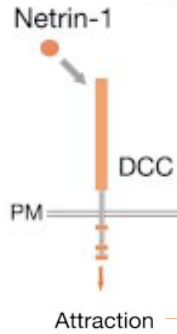
Netrin-1 gradient

DCC

DCC-UNC5

Netrin-1

DCC   UNC5   DCC

PM

Attraction   Repulsion

Nishiyama et. al, Nature (2003)

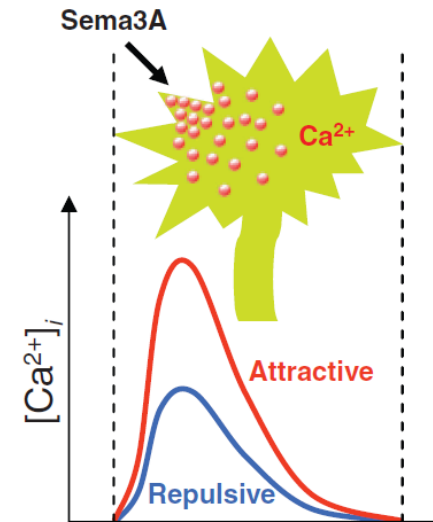# cAMP/cGMP controls bidirectional responses of the growth cone

Nishiyama et. al, Nature (2003)   Total concentration is fixed at 10μM.

Gradient direction is encoded into steepness or basal concentration of Ca2+

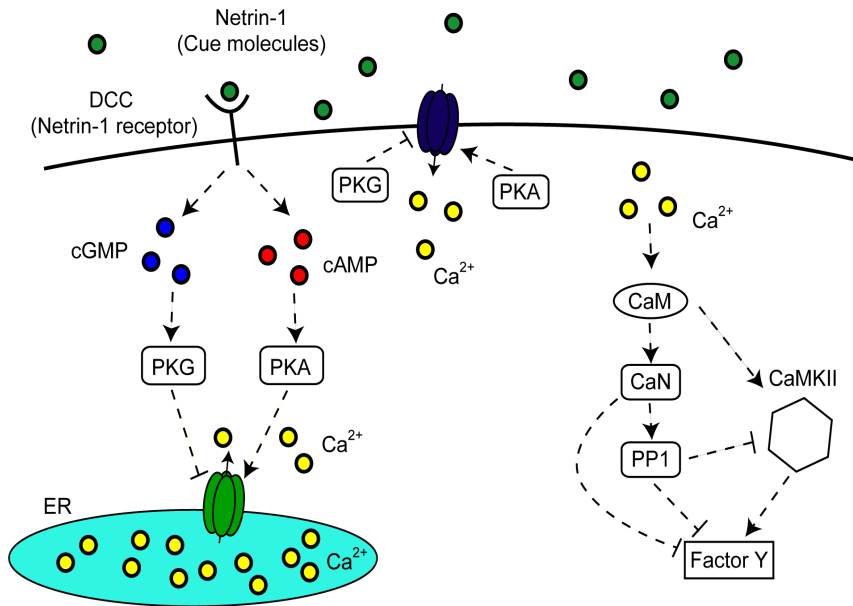**Ca2+ imaging with Sema3A gradient**
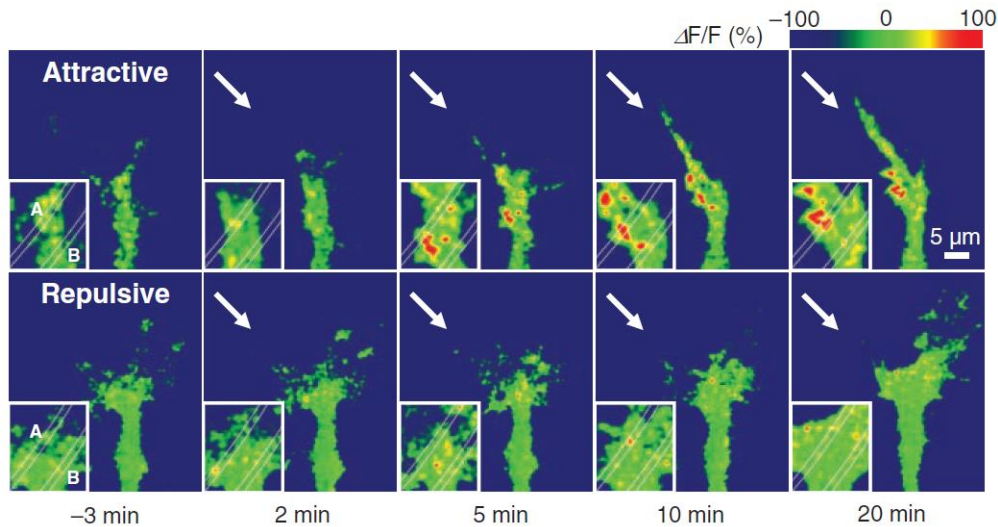
Nishiyama et al., Nat Neurosci (2008)

During attraction, a 2-fold greater Ca2+ increase is induced than are induced by repulsive signals.


Questions

- How gradient information is encoded into Ca2+?
- How Ca2+ signal is decoded by downstream cascade?

A combined activator-inhibitor model

Netrin-1
(Cue molecules)

DCC
(Netrin-1 receptor)

PKG   PKA

cGMP   cAMP   Ca²⁺   Ca²⁺

PKG   PKA   CaM

Ca²⁺   CaN   CaMKII

ER   PP1

Ca²⁺   Factor Y

(Guidance Cue)

G

Extracell

Intracell

I   A

(Inhibitor)   (Activator)

X

(Factor X)

• In this growth cone turning system, there are two kinds of balancing factors between activator and inhibitor.
  • Upstream of Calcium
    • cAMP (A) vs. cGMP (I)
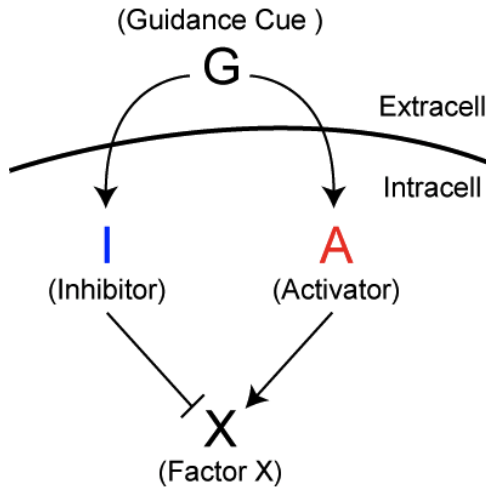 • Downstream of Calcium
    • CaMKII (A) vs. CaN-PP1 (I)
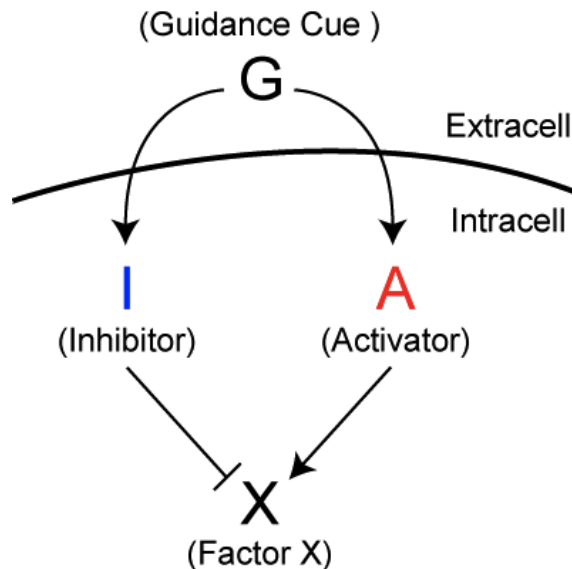
Reaction-diffusion equation

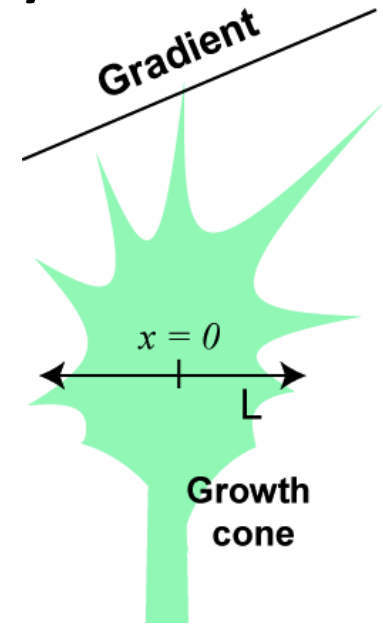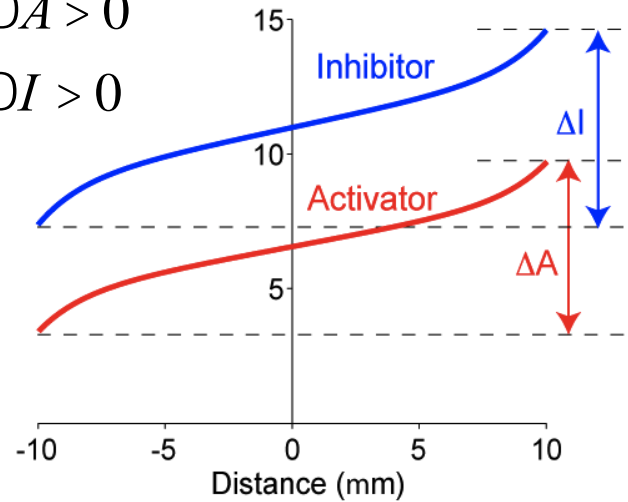$$\frac{\partial A}{\partial t} = D_A \frac{\partial^2 A}{\partial x^2} + f_A\left(A; G(x)\right)$$

$$\frac{\partial I}{\partial t} = D_I \frac{\partial^2 I}{\partial x^2} + f_I\left(I; G(x)\right)$$

Mathematics: an activator-inhibitor system can exhibit bidirectionality

$DA > 0$
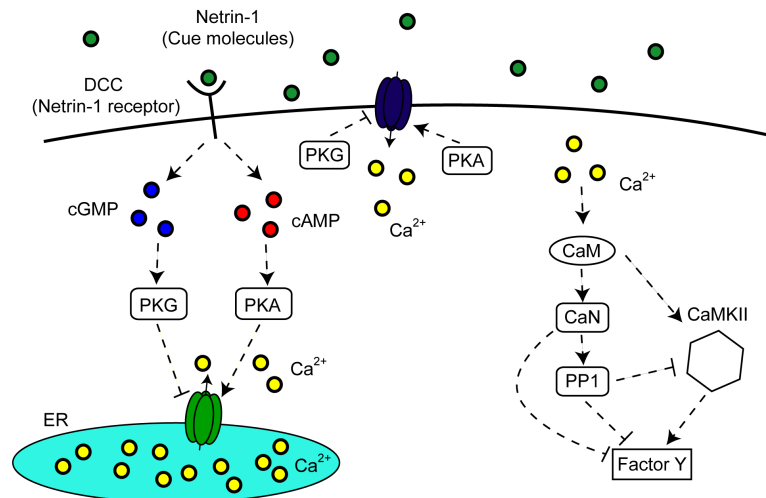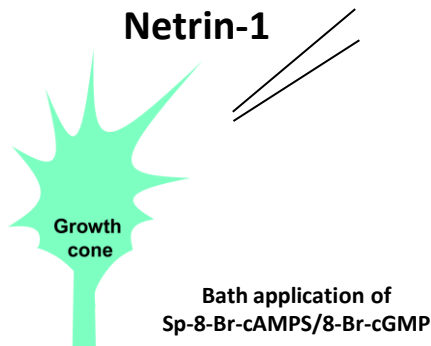
$DI > 0$

Spatial difference of X across the growth cone
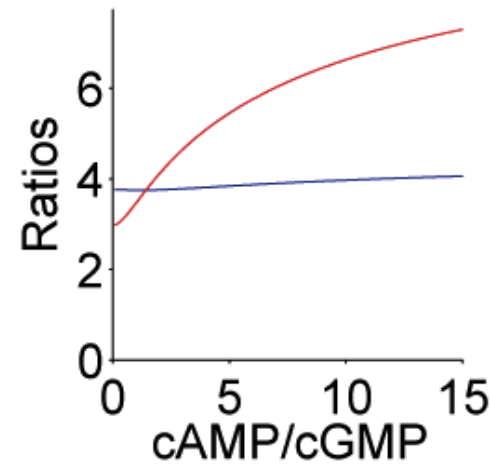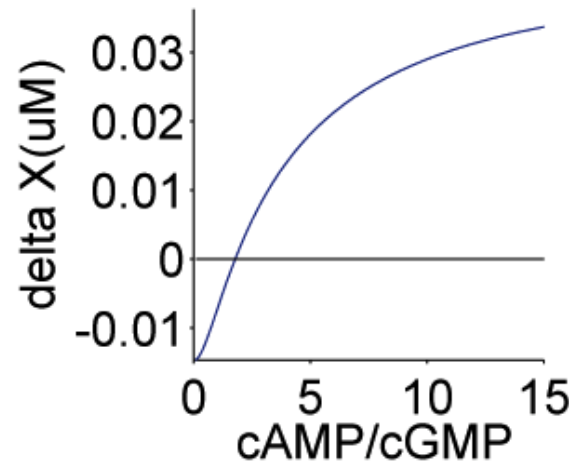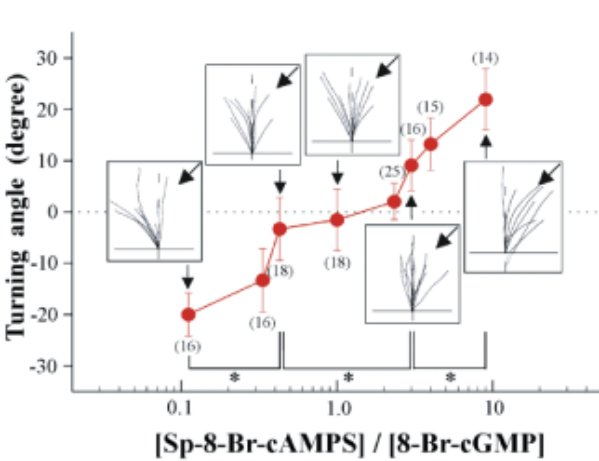
$$DX \equiv X(L/2) - X(-L/2) = \left.\frac{dh_X}{d(A/I)}\right|_{\frac{A^*}{I^*}} \frac{A^*}{I^*}\left(\frac{DA}{A^*} - \frac{DI}{I^*}\right)$$

Repulsive condition (ΔX<0)
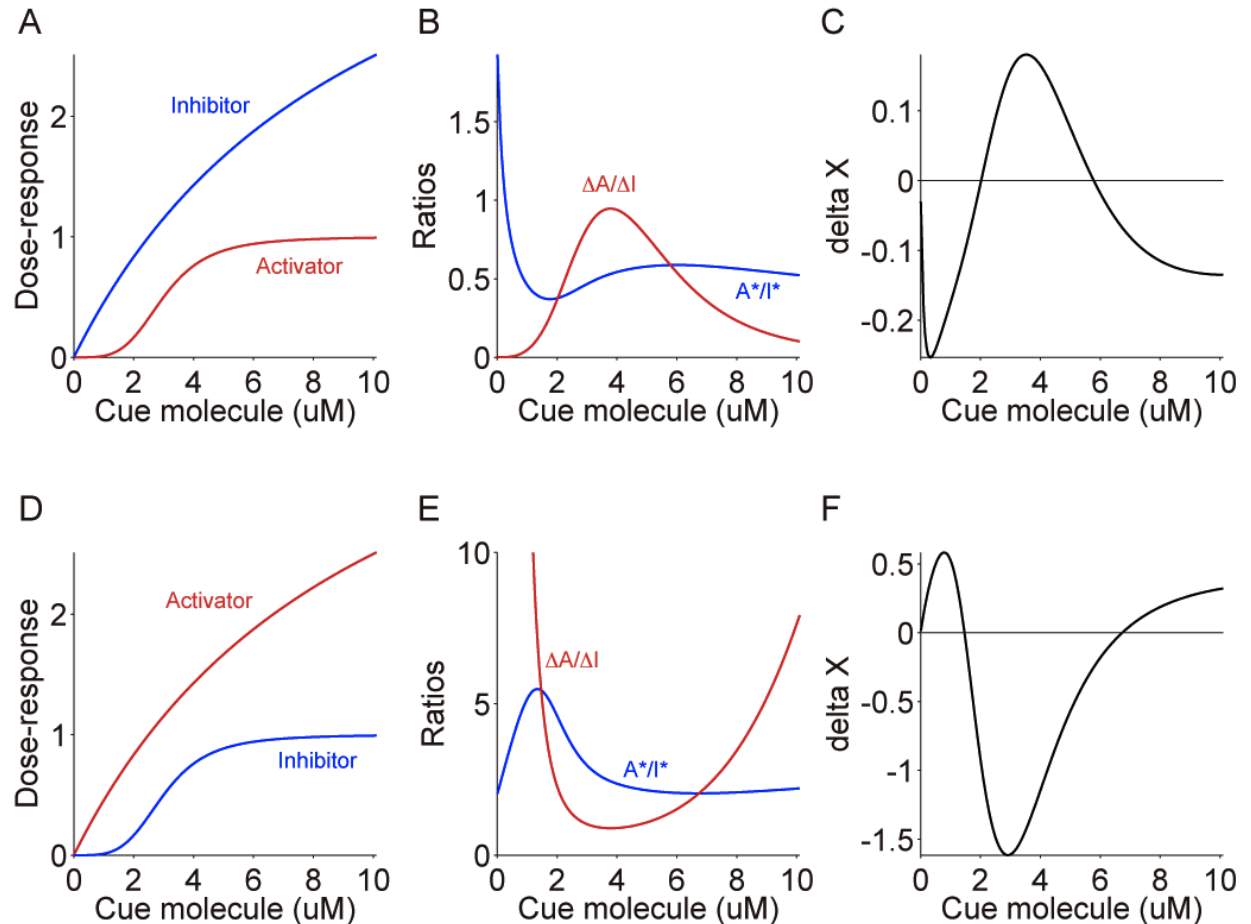
$$\frac{A^*}{I^*} > \frac{DA}{DI}$$

Magnitude relation between A^*/I^* and $\Delta A/\Delta I$ determines attractive or repulsive turnings.

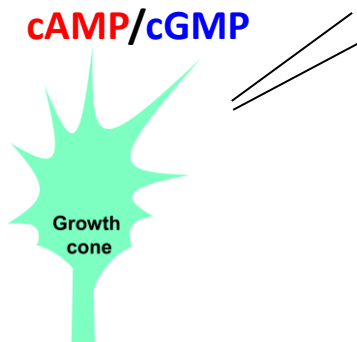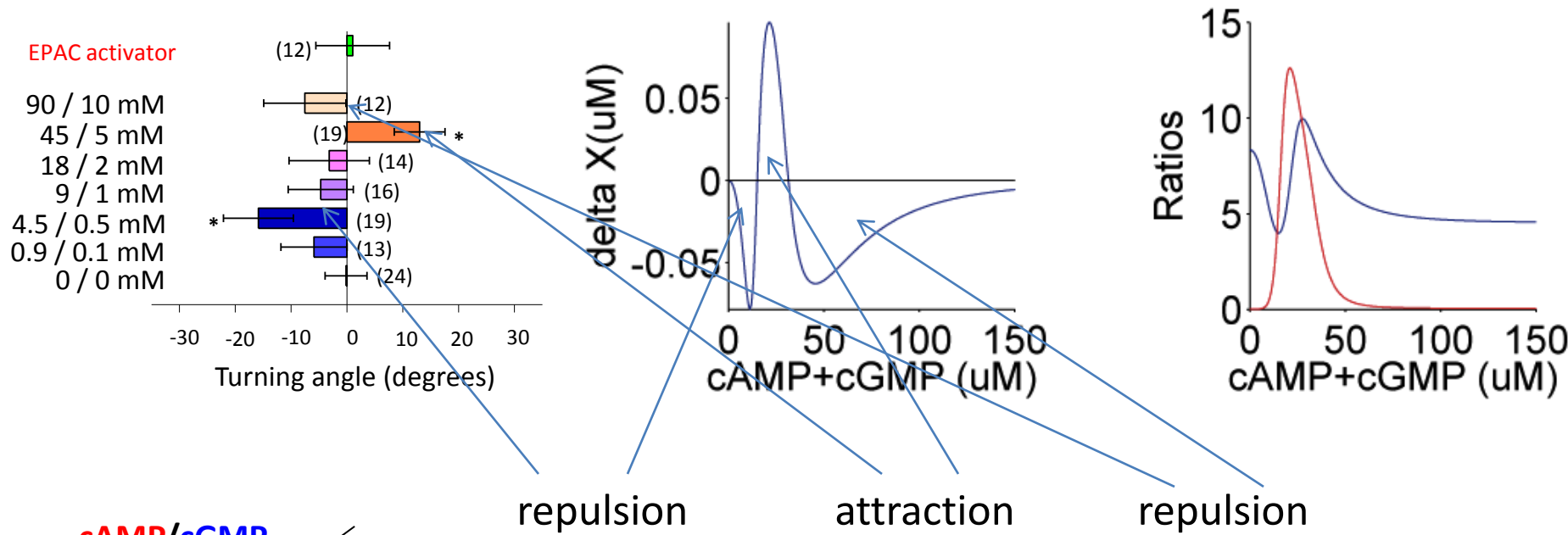# The mathematical model can reproduce bidirectional responses

The mathematical model further predicts more complicated behaviors

When the activator and inhibitor are upregulated in a **non-linear** manner,...

The predicted complicated behaviors are experimentally confirmed

EPAC activator

90 / 10 mM (12)
45 / 5 mM (12)
18 / 2 mM (19) *
9 / 1 mM (14)
4.5 / 0.5 mM (16)
0.9 / 0.1 mM (19) *
0 / 0 mM (13)
(24)

Turning angle (degrees)
-30 -20 -10 0 10 20 30

delta X(uM)
0.05
0
-0.05
cAMP+cGMP (uM)
0 50 100 150

Ratios
15
10
5
0
cAMP+cGMP (uM)
0 50 100 150

repulsion   attraction   repulsion

cAMP/cGMP

Growth cone

When the activator/inhibitor exhibits non-linear responses, the system's response become complicated.
This kind of nonlinearity may be used for situation-dependent growth cone guidance in developing neurons.

Large-scale simulation of neural systems, in Japan

Diesmann, M., Fukai, T., Usui, S., Kuroda, S., Ichikawa, K.,
Kanzaki, R., Doya, K., Ishii, S.,
and many young researchers

Japanese supercomputer K achieved the world fastest (20, June, 2011)

LINPACK performance:
8.162 PFLOPS
(548, 352 cores)
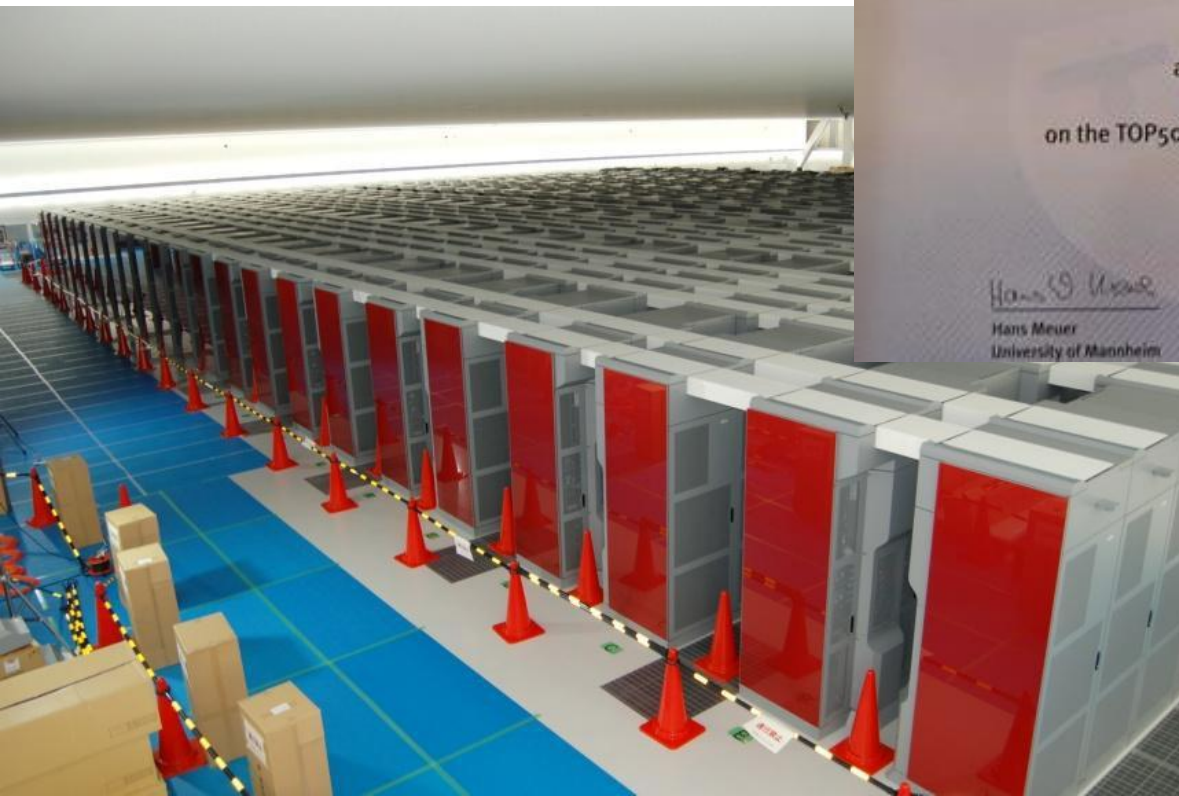
"K" comes from the Japanese word "Kei " which means ten peta or 10 to the 16th power.

K supercomputer outlook

- Over 80,000 processors
  - Over 640K cores
  - Over 1 Peta Bytes memory
- Cutting-edge technologies
  - CPU: SPARC64 VIIIfx, 8 cores, 128GFlops
  - Interconnect, "Tofu": 6-D mesh/torus
 - Parallel programming environment

CPU (SPARC64 VIIIfx)	Cores/Node	8 cores (@2GHz)
	Performance	128GFlops
	Architecture	SPARC V9 + HPC extension
	Cache	L1(I/D) Cache : 32KB/32KB L2 Cache : 6MB
	Power	58W (typ. 30 C)
	Mem. bandwidth	64GB/s.
Node	Configuration	1 CPU / Node
	Memory capacity	16GB (2GB/core)
System board(SB)	No. of nodes	4 nodes /SB
Rack	No. of SB	24 SBs/rack
System	Nodes/system	> 80,000

Inter-connect	Topology	6D Mesh/Torus
	Performance	5GB/s. for each link
	No. of link	10 links/ node
	Additional feature	H/W barrier, reduction
	Architecture	Routing chip structure (no outside switch box)
Cooling	CPU, ICC*	Direct water cooling
	Other parts	Air cooling

http://www.fujitsu.com/downloads/TC/sc10/when-high-performance-computing-meets-energy-efficiency.pdf

Grand challenge: Next generation integrated simulation of living matter

- Promote the research and development of simulation software which helps **understand phenomena from molecules to entire organisms**

- Long-term "grand challenges" aimed at the construction of a basis for future life science unifying experiments and computer simulations to gain new knowledge for the first time.
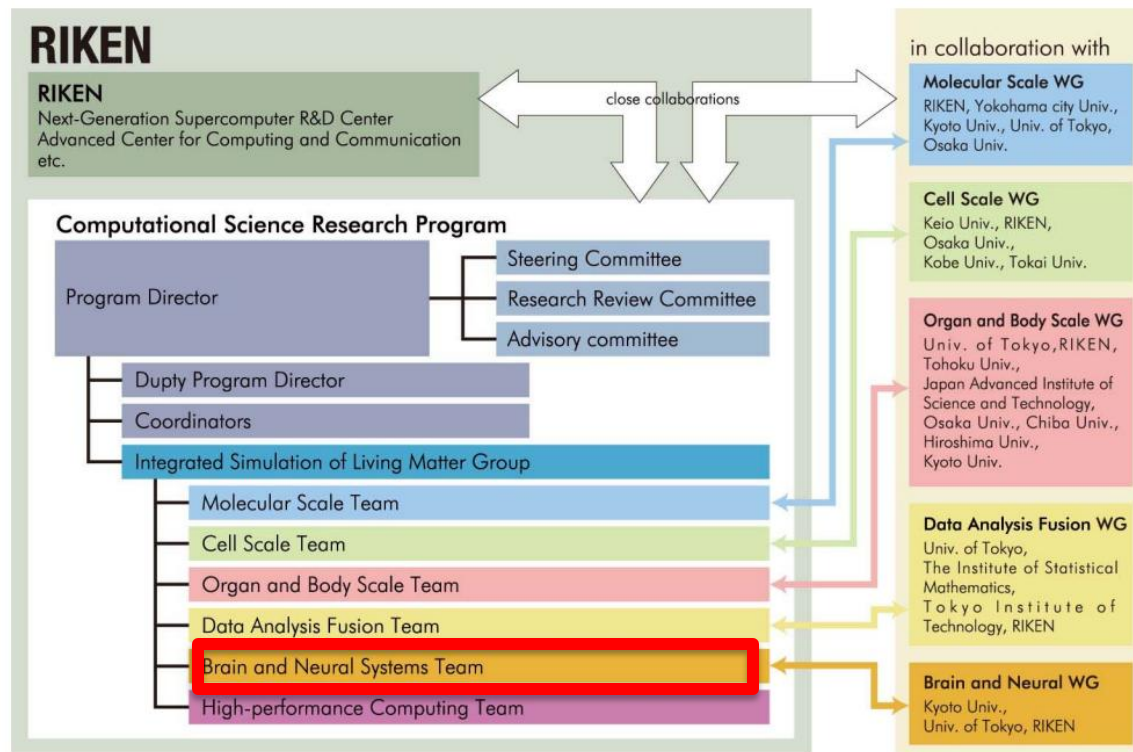
http://www.csrp.riken.jp/index_e.html

# Software: neuron and circuits simulators

NeuroMorphoKit

C, C++, MPI, OpenMP, GSL, NetCDF, GD, zlib

A multiphysics simulation environment for neuromorphological dynamics

is a software platform for neuronal morphological simulation by integration of kinetics of cytoskeletal filaments, cell membrane dynamics, and reaction-diffusion of intracellular molecules
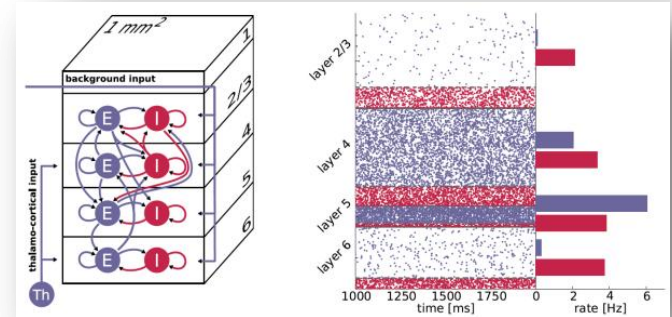
Shin Ishii

Kazuhisa Ichikawa
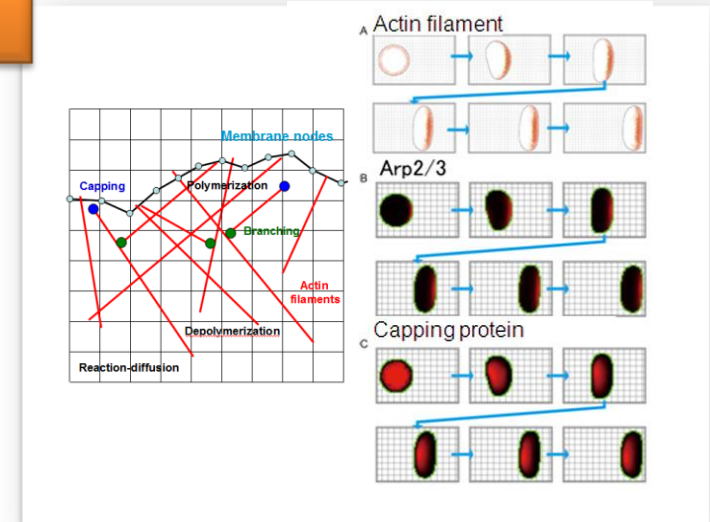
NEST

C++, SLI, MPI, pthread

Neural Simulation Tool

simulates and predicts the signal processing for 10 million neurons equivalent to 100 columns in the cortex, and 100 billion synapses connecting the neurons

Markus Diesmann

Tomoki Fukai

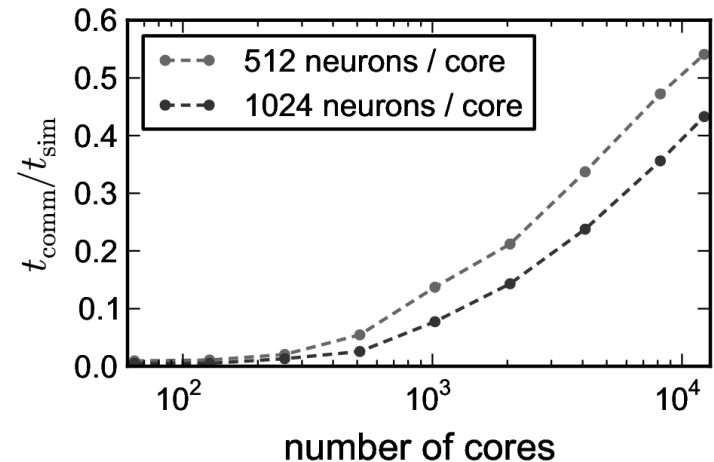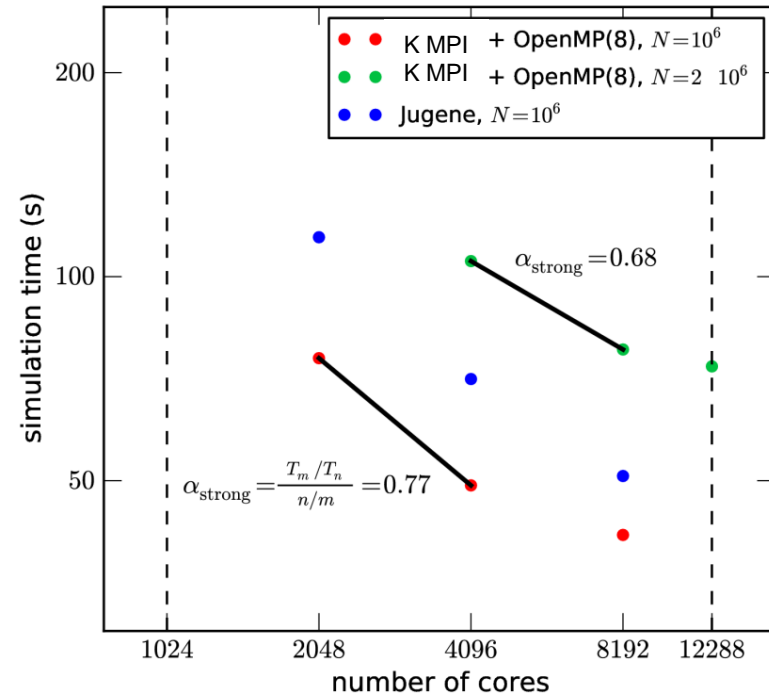# Neural Simulation Tool (NEST) on K

- ## Now available on K

  - high degree of parallelization is achieved by using hybrid MPI + OpenMP threads with more than 8000 cores on K supercomputer

  - very good scaling up to 4096 cores, speedup α > 0.75

  - good scaling for > 8000 cores, speedup α = 0.68

- ## Action plan

  - Employ computer's specific optimizations of NEST code

  - improves communication computation balance

NEST STDP benchmark, $K = 10^4$

$\alpha_{strong} = 0.68$

$\alpha_{strong} = \frac{T_m / T_n}{n/m} = 0.77$

K MPI + OpenMP(8), $N = 10^6$
K MPI + OpenMP(8), $N = 2 \cdot 10^6$
Jugene, $N = 10^6$

simulation time (s)
number of cores

t_{comm}/t_{sim}

512 neurons / core
1024 neurons / core

number of cores

Software: whole-brain level circuits

VSM
C, C++, OpenMPI, GSL, netCDF

The visual information processing analysis with a whole visual system model

targets the visual system being built with the mathematical model that is described in each level of function, cell, and ion current for cortex, retina, ophthalmological optics, and eye motion (brainstem)
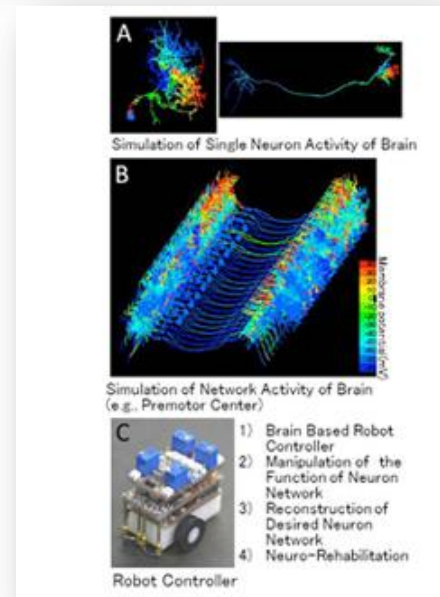
Shiro Ushi, Kenji Doya
Shinya Kuroda
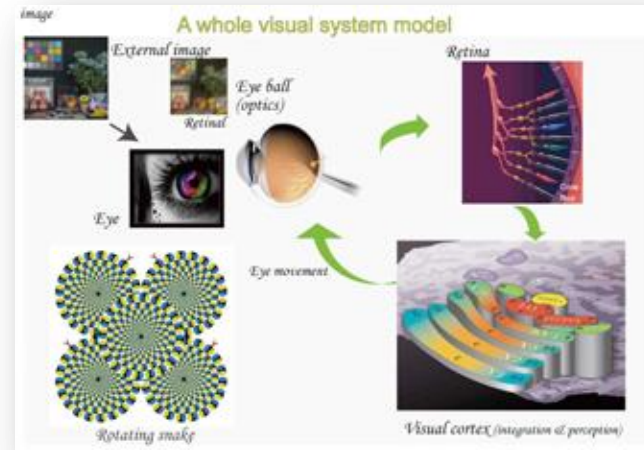
IOSSIM
C, C++, MPI, SUNDIAL InterView

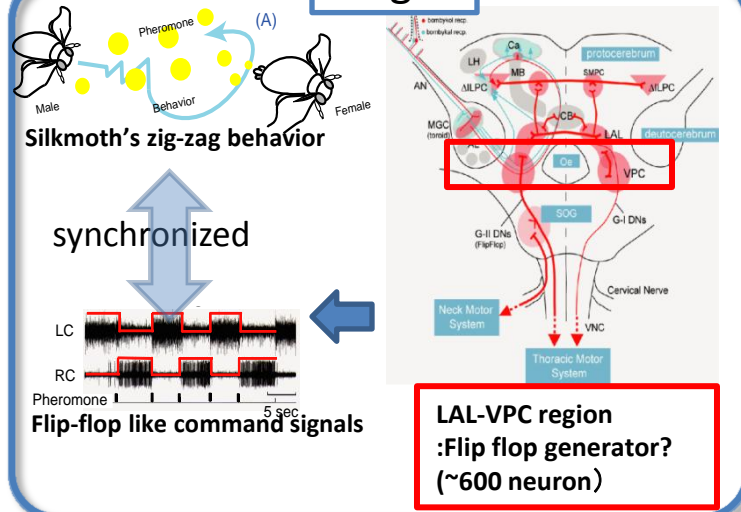Whole-brain simulator for the insect's olfactory system

performs a virtual-spatial real-time simulation for the neural circuit's information processing of an insect from sensing to action by the multi-compartment model that considers each neural configuration
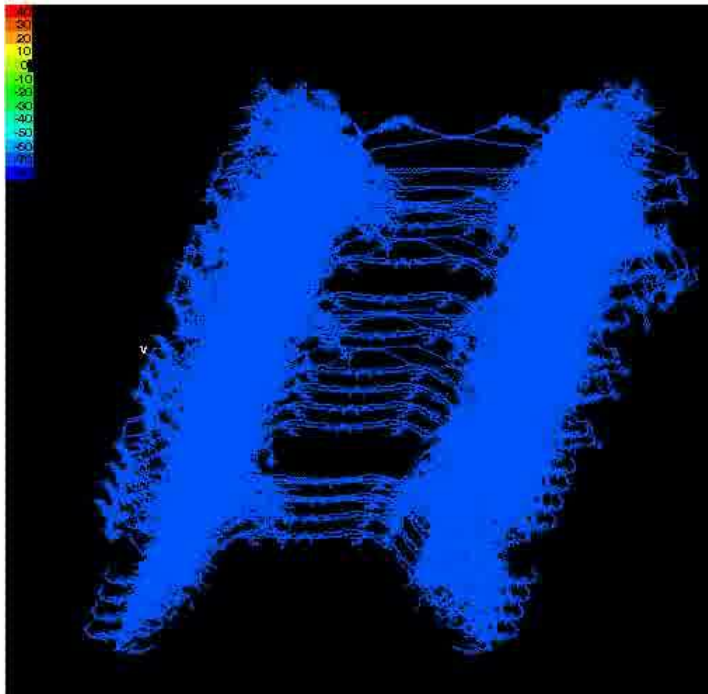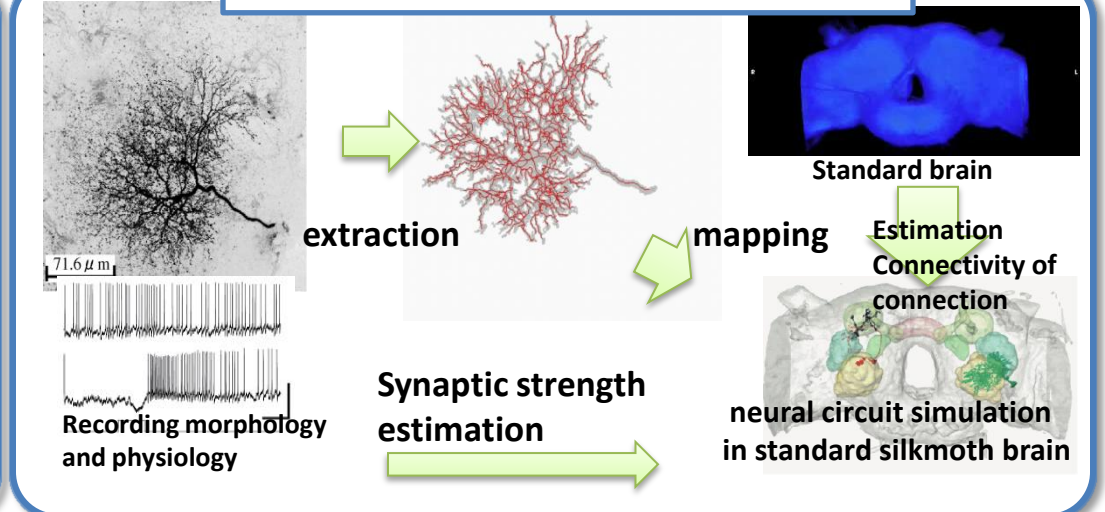
Ryohei Kanzaki

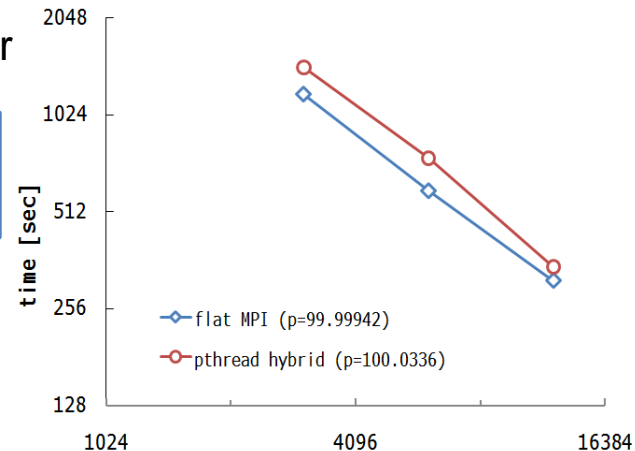# Large-scale simulation of insects' whole olfactory system (IOSSIM)

Target

Silkmoth's zig-zag behavior

synchronized

Flip-flop like command signals

LC
RC
Pheromone
5 sec

LAL-VPC region
:Flip flop generator?
(~600 neuron）

Methods to construct simulation

extraction

71.6 μm

Recording morphology and physiology

mapping

Standard brain

Estimation Connectivity of connection

Synaptic strength estimation

neural circuit simulation in standard silkmoth brain

- Multi-compartment H-H neurons
- 72 neurons, 12900 synapses
- Inhibitory linter-neurons and excitatory bilateral neurons
- Synaptic connections based on morphological analysis of the LAL-VPC circuit
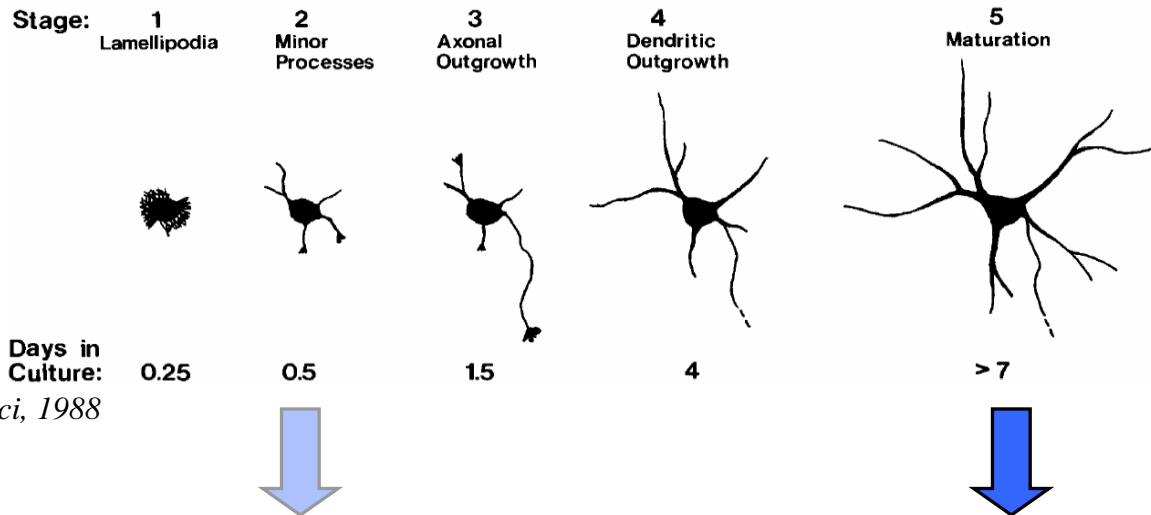- Working on K computer

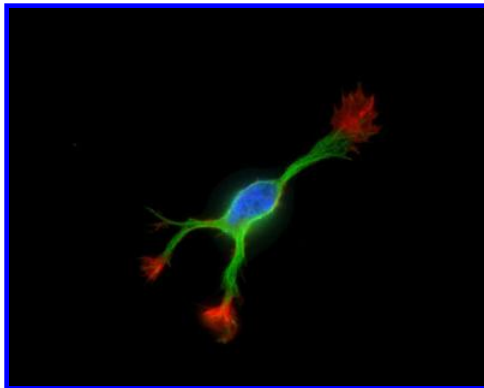Large-scale simulation on K supercomputer

time [sec]

flat MPI (p=99.99942)
pthread hybrid (p=100.0336)

2048
1024
512
256
128

1024   4096   16384

Cytoskeleton-based morphogenesis: a multi-physics simulation

Nonaka, S., Naoki, H., Ishii, S. Neural Networks, 2011.
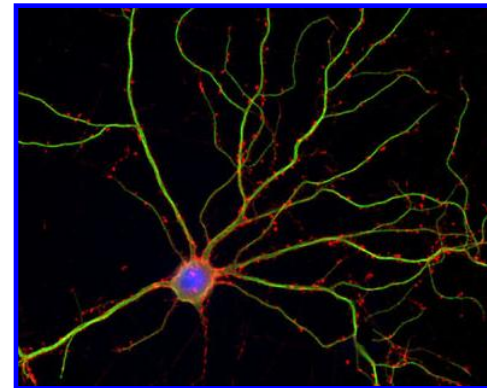
Cytoskeleton in neuronal morphogenesis

Dotti et. al, J Neurosci, 1988

Actin filament
Microtubule

Neurites:
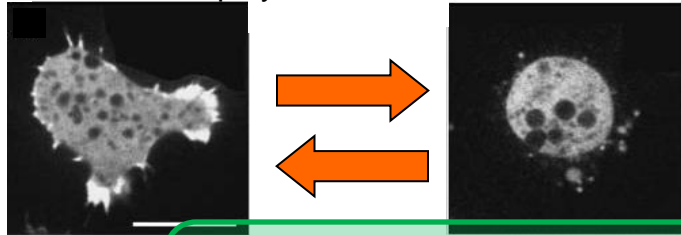**Actin** and **Microtubule** are localized
at tips and along shafts, respectively.

Dendrite / Synapses:
Actin and **Microtubule** are localized
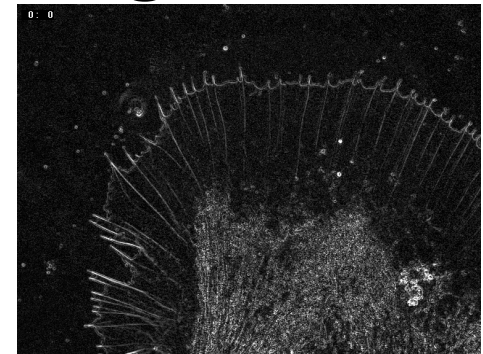at synapses and along dendritic shafts, respectively.

Cytoskeleton, especially actin, is involved in structural plasticity.

Multi-physics in cellular morphogenesis

Actin polymerization inhibitor

Gerisch, et al., Biophys J, 2004

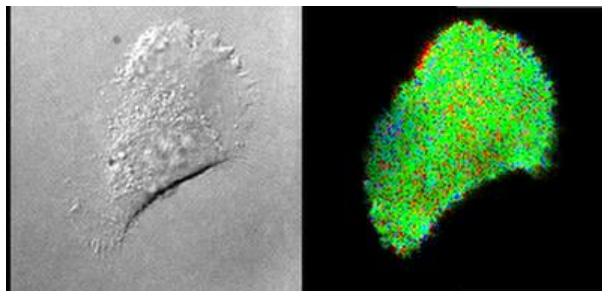(by Dr. Kaoru Katoh)

Membrane
Deformation and motility

Mechanically sustain membrane

Cytoskeleton (actin)
Polymerization, blanching, etc

Boundary conditions for reaction-diffusion

Kinetics control

Intracellular signaling
Reaction-diffusion

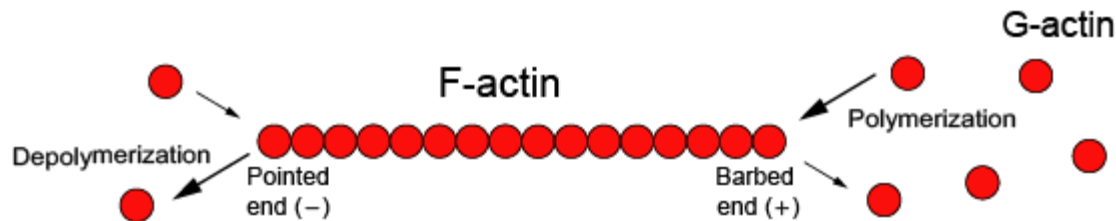**Cdc42**-FRET imaging in fibroblast *by Matsuda lab*
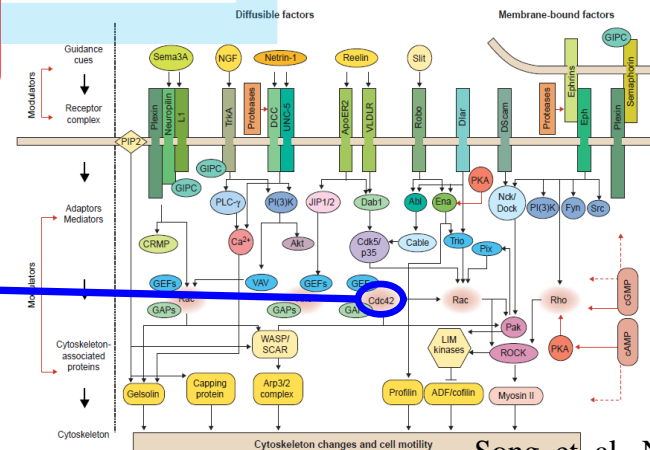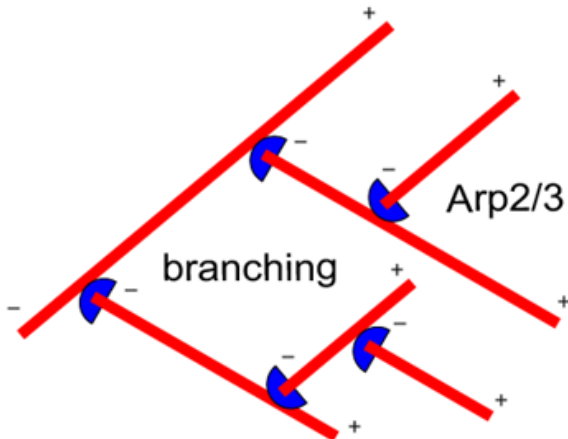
Song, et. al., Nat Cell Biol, 2001

Actin filaments control cell motility

Polymerization and de-polymerization
Treadmilling

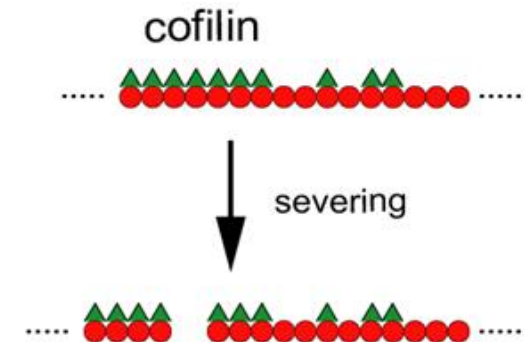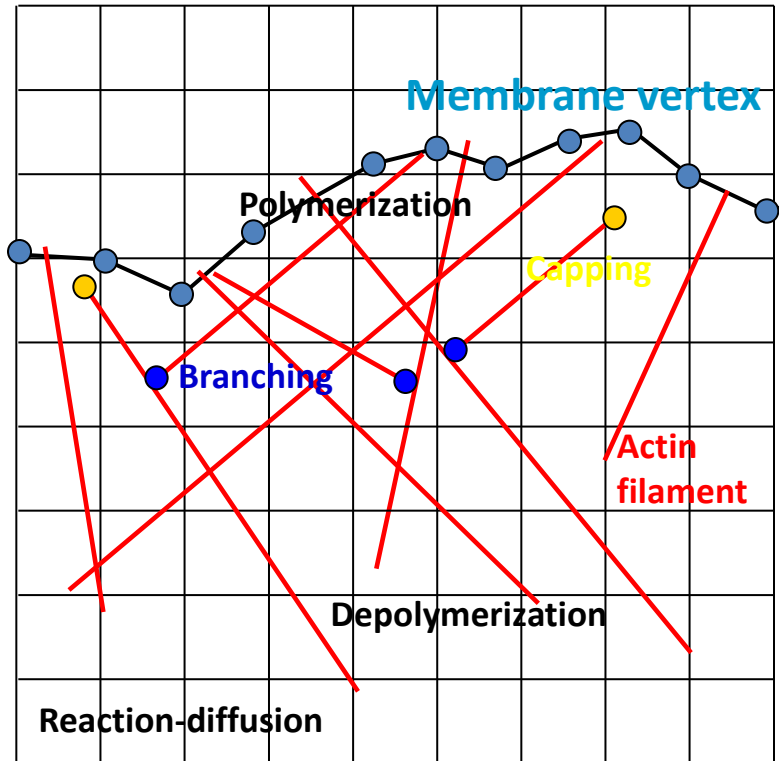Actin treadmill would provide driving force for cell motility

Branching
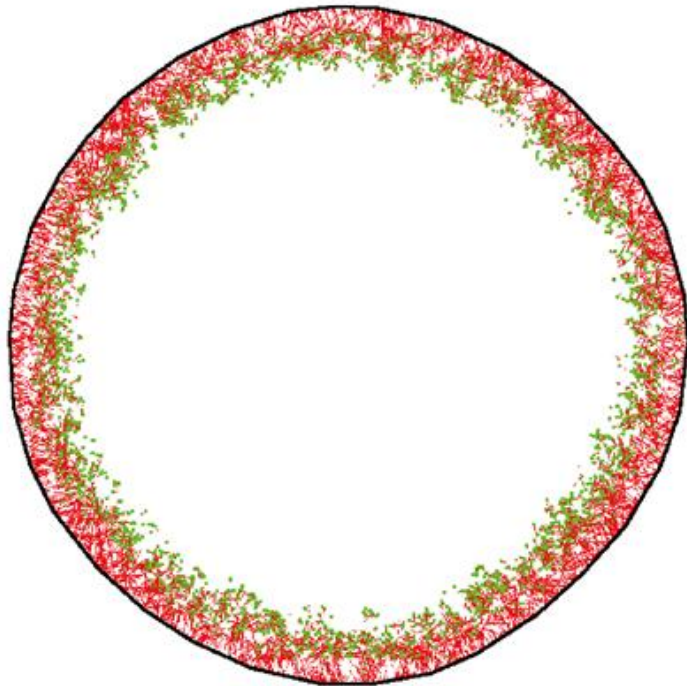
Capping

Severing

# Compartment model of multi-physics

Within each step (Δt)

Membrane vertex

Polymerization

Capping

Branching

Actin filament

Depolymerization

Reaction-diffusion

Intracellular signaling
Reaction-diffusion

⬇

Cytoskeleton (actin)
Actin filament reorganization

⬇

Membrane
Energy-based deformation
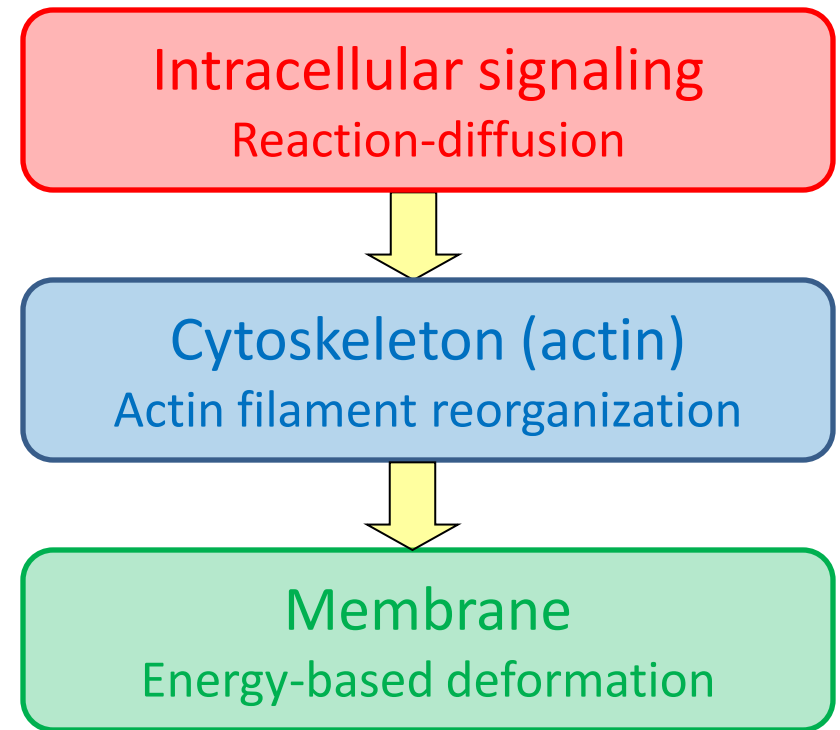
- Space is compartmentalized.
- Membrane is expressed by polygon.
- Actin filament is expressed by line segments.

Neuroinformatics 2011

Simulation: self-organization of lamellipodia

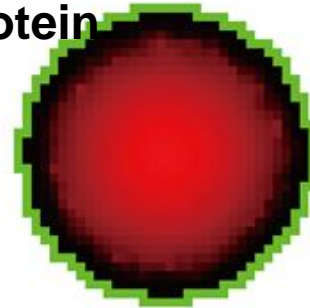**Actin filament**
Capping protein

Active Arp2/3
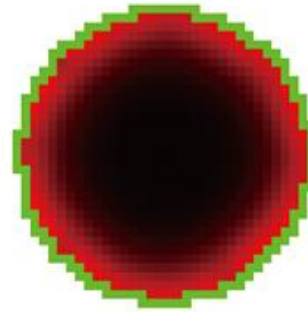
- Arp2/3 is activated in the vicinity of the membrane.

  Blanchoin, et. al, Biophy J, 2005
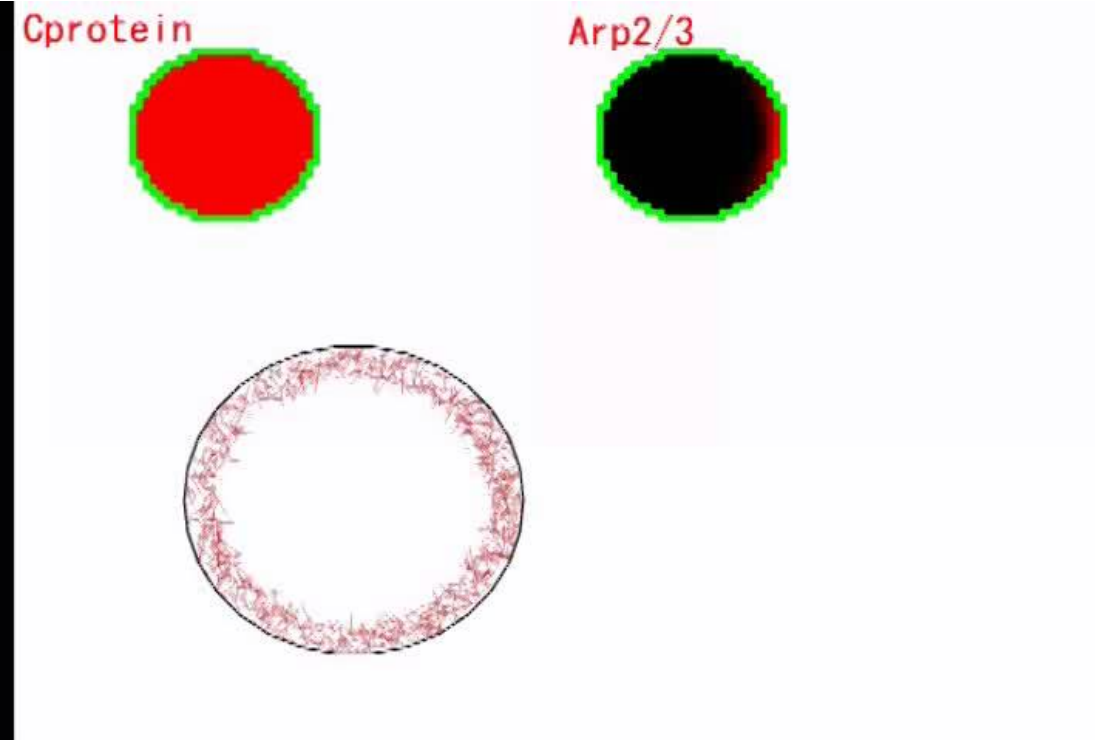
Active Capping protein

- Capping protein is inactivated in the vicinity of the membrane.

  Bear, et. al, Cell, 2002
  Schafer, et. al, J Cell Biol, 1996

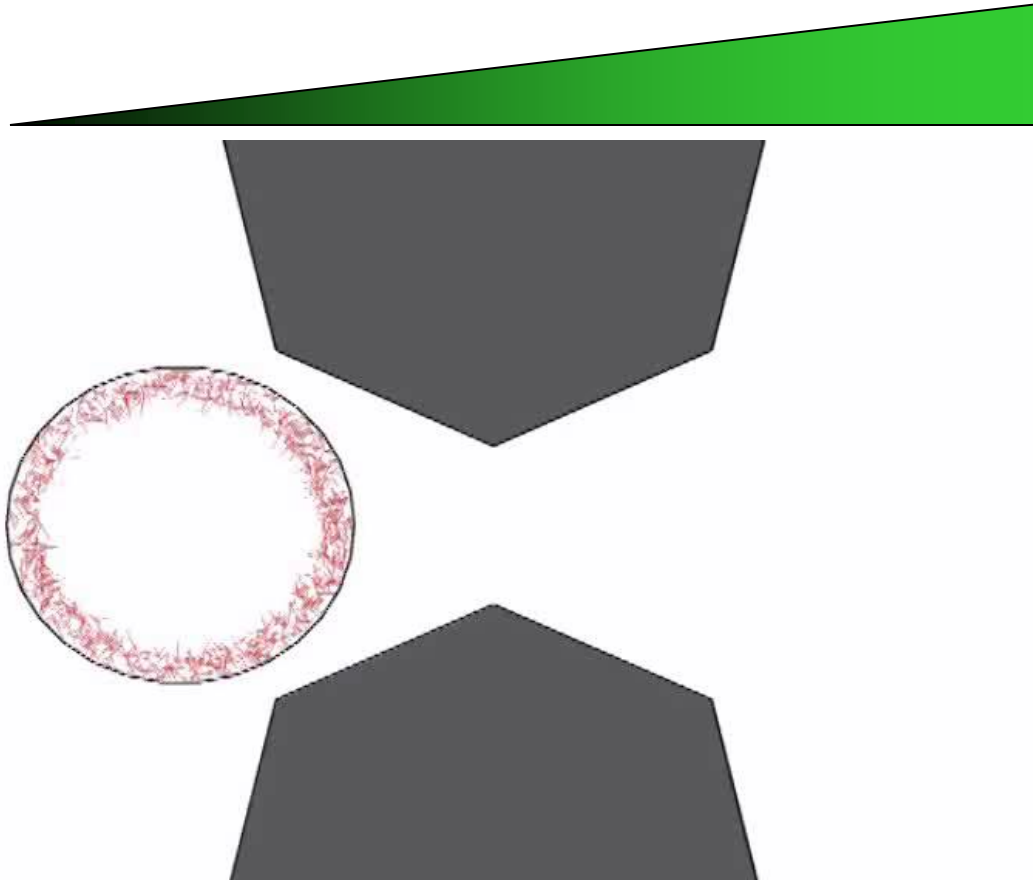Meshed network of actin filament is organized.
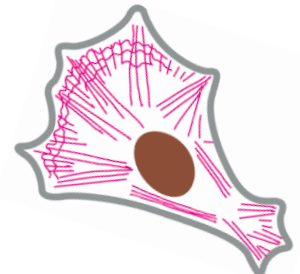
Simulation: chemotactic migration

Chemo-attractant gradient

- Chemo-attractant activates receptor.
- Activated receptor activates Arp2/3 complex.

Simulation: invasive migration
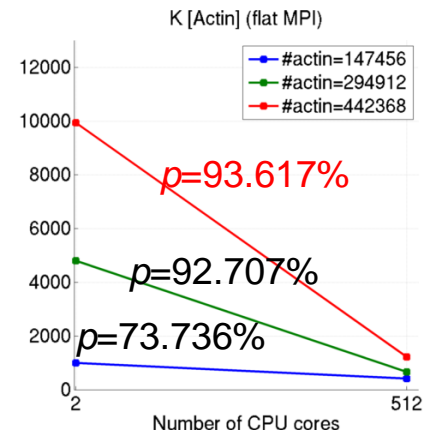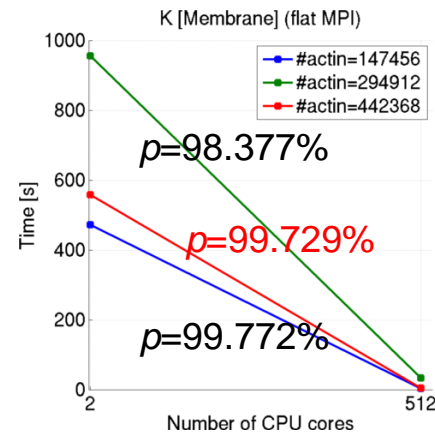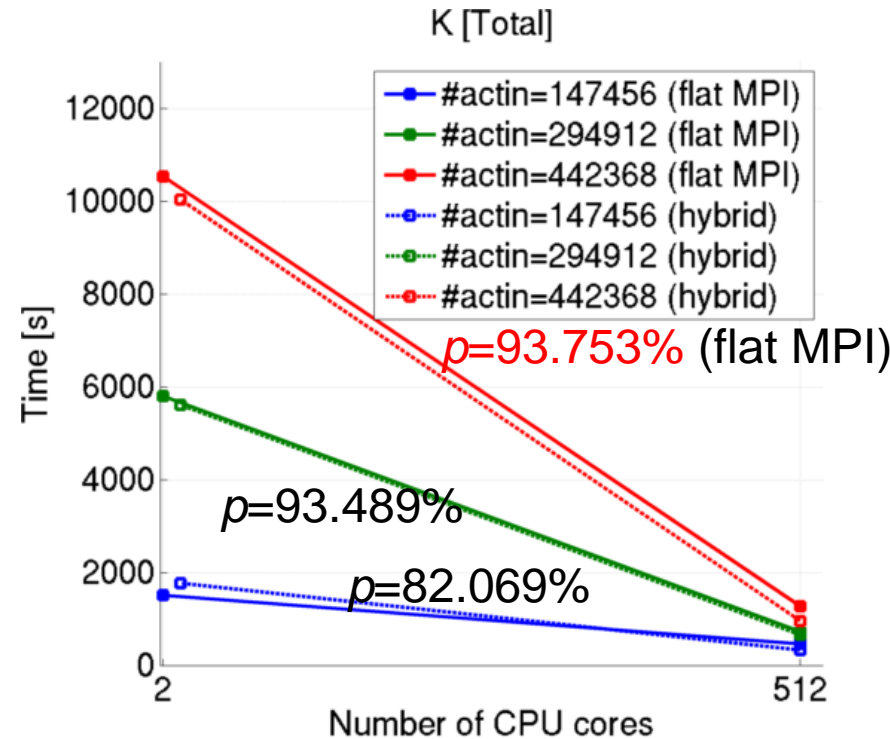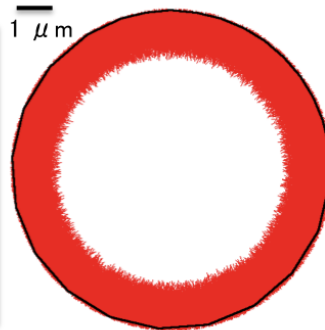

Chemo-attractant gradient

- Locate obstacles, which correspond to other cells or extra-cellular matrix.
- Energy optimization is performed with a constraint such that the membrane vertices are not overlapped with the obstacles.
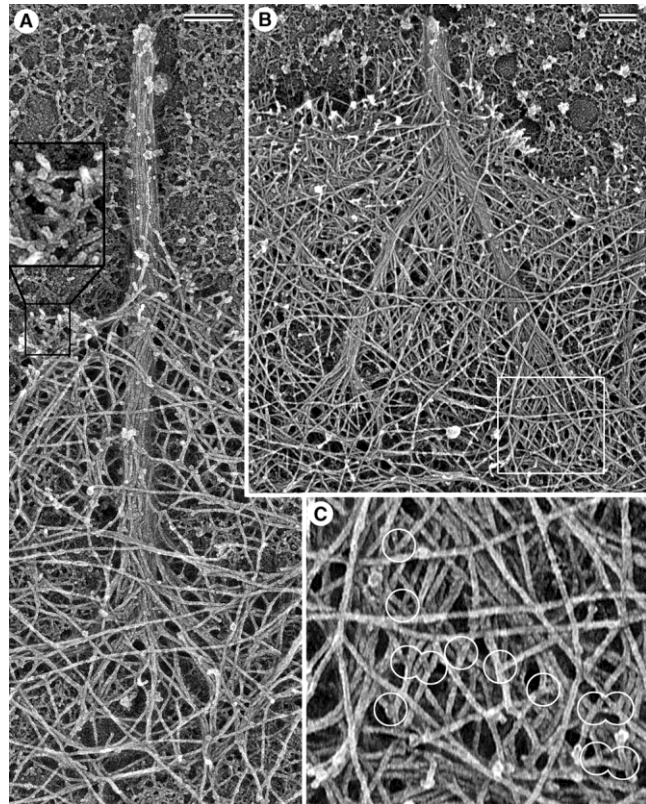
Simulation on K supercomputer

- ## Current status
  - tested up to 512 cores
  - hybrid of MPI and OpenMP enabled more efficient computations on larger scale settings
  - accomplished moderate parallelization on the membrane energy optimization (p=99.729%)

K [Total]

Legend:
- #actin=147456 (flat MPI)
- #actin=294912 (flat MPI)
- #actin=442368 (flat MPI)
- #actin=147456 (hybrid)
- #actin=294912 (hybrid)
- #actin=442368 (hybrid)

Time [s] (axis: 0, 2000, 4000, 6000, 8000, 10000, 12000)

p=93.753% (flat MPI)

p=93.489%

p=82.069%

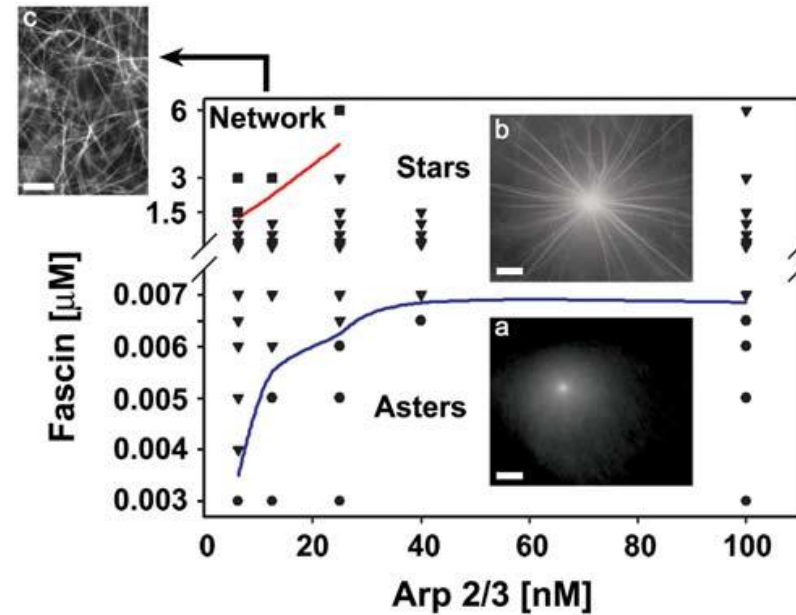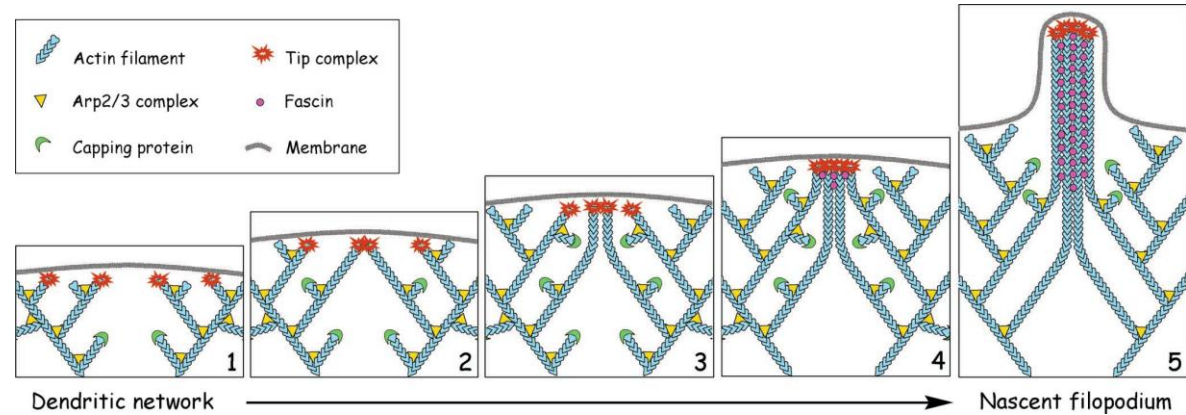Number of CPU cores (2 to 512)

Simulation setup
- initial number of actin filaments > 10^6
  - small: 147456
  - middle: 294912
  - large: 442368
- initial number of membrane nodes
- 1200 ms biological time simulation

1 μm

K [Membrane] (flat MPI)

Legend:
- #actin=147456
- #actin=294912
- #actin=442368

Time [s] (axis: 0, 200, 400, 600, 800, 1000)

p=98.377%

p=99.729%

p=99.772%

Number of CPU cores (2 to 512)

K [Actin] (flat MPI)

Legend:
- #actin=147456
- #actin=294912
- #actin=442368

(axis: 2000, 4000, 6000, 8000, 10000, 12000)

p=93.617%

p=92.707%

p=73.736%

Number of CPU cores (2 to 512)

Bendable F-action and linker protein are required for filopodial formation

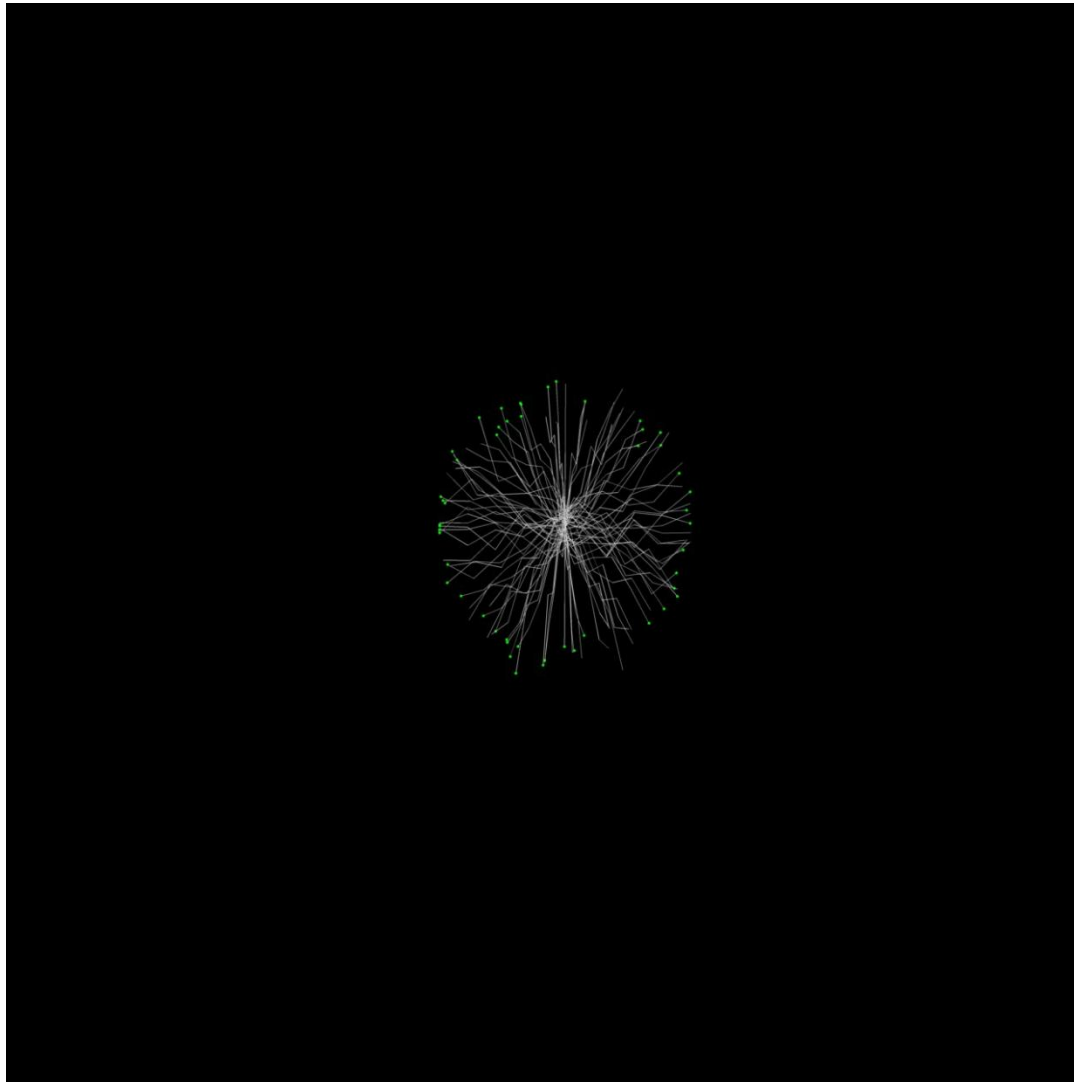Svitkina *et al*., J Cell Biol, 2003

Filopodia-like structure appears in a membrane-free environment only with actin, Arp2/3 and fascin.

Ideses *et al*., PLoS ONE, 2008

Simulation of *in vitro* reconstruction of filopodia

Star-like structure of filopodia is self-organized

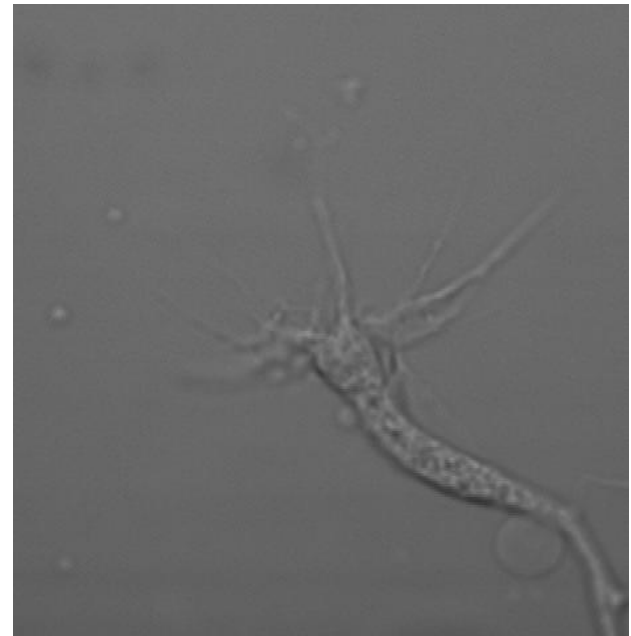While line: bendable F-actin   Red point: fascin

Future: from modeling to decoding

In house

Brain Machine Interface
(decoding from the brain)

In vivo

Growth-cone Machine Interface?
(decoding from neurons and growth cones)

Summary

- Information processing in neuronal morphogenesis
  - Neuronal polarization
  - High SNR in chemotaxis
  - Bidirectional responses by growth cones
- Large-scale simulations of neural systems
  - Large-scale simulation studies in Japan
  - Multi-physics simulation of neuronal morphogenesis
    - Lamellipodia formation and cell migration
    - Bendable F-actin and filopodia formation